QTL Mapping and GWAS Identify Sources of Iron Deficiency Chlorosis and Canopy Wilt Tolerance in the Fiskeby III X Mandarin (Ottawa) Soybean Population

A Thesis

SUBMITTED TO THE FACULTY OF THE GRADUATE SCHOOL

OF THE UNIVERSITY OF MINNESOTA

BY

Karl Joseph Butenhoff

IN PARTIAL FULFILLMENT OF THE REQUIREMENTS

FOR THE DEGREE OF

MASTER OF SCIENCE

Advisor, James Orf

January 2015

Acknowledgements

I am foremost grateful to my advisor, Dr. James Orf, for his commitment to teaching and mentorship during my time at the University of Minnesota. I deeply appreciate the opportunity I had to learn from and work with him throughout my undergraduate and graduate careers. I am also thankful to my advisory committee, Drs. Seth Naeve and Robert Stupar, for their insights and review of this thesis. I would also like to thank all of my instructors at the University of Minnesota who have helped me during my degree to grow as a student, scientist, and individual.

I am deeply grateful for the guidance, assistance, and friendship of fellow graduate students Yong Bao, Jared Goplen, Amy Jacobson, Wade Kent, Tom Kono, Josh Sleper, and Eric Wilson. I also would like to thank Amy Burton, Tommy Carter, and Kent Burkey of the United States Department of Agriculture for creating the mapping population used in this project and for their support throughout my research. In addition, I owe many thanks to the members of the soybean breeding project because without their help this research could not have been completed.

I am also thankful for the support of my friends and family during my time in graduate school, especially from my parents, Al and Jackie. Finally, I would like to thank Sarah Eichenberg for her constant love and the incredible support she provides for all that I do.

Abstract

Abiotic stresses are a major yield limiting component in soybean production that producers cannot directly control. Therefore, an increase in the understanding of how different abiotic stresses affect soybean, and the identification of sources of tolerance to these stresses will be critical for the continued increase of soybean productivity well into the future. Here I present three separate, but related, studies analyzing iron deficiency chlorosis and drought tolerance in several soybean populations. For the first and second studies, the objectives were to (i) characterize the Fiskeby III X Mandarin (Ottawa) recombinant inbred line (RIL) population for its tolerance to iron deficiency chlorosis (IDC) and drought; (ii) identify quantitative trait loci (QTL) via composite interval mapping for iron deficiency chlorosis and canopy wilt in the RIL population; and (iii) identify co-localization of abiotic stress QTL and putative candidate genes for iron deficiency chlorosis tolerance and delayed canopy wilt. Iron chlorosis and canopy wilt scores were significantly different across the three years tested between the RILs as well as the parents of the population. Fiskeby III consistently scored better than Mandarin (Ottawa) for tolerance to iron chlorosis and canopy wilt in all three years. Two QTL were discovered, one on chromosome five and one on chromosome six, that together accounted for approximately 25 percent of the phenotypic variation for IDC. Two QTL were also identified for canopy wilt, one on chromosome six and one on chromosome 12, that together accounted for approximately 13 percent of the phenotypic variation. The two QTL identified on chromosome six co-localized to the same confidence interval. Several previously identified QTL co-localized with the identified IDC and canopy wilt QTL in this study. In addition, a potential candidate gene was identified on chromosome

five that may play a role in the soybean IDC response. The third study was undertaken to potentially validate the QTL identified for IDC in the first study in two independent soybean populations. The objectives of this study were to (i) utilize association mapping to detect markers significantly associated with IDC in two independent populations, (ii) compare significant identified markers with the QTL regions identified in the bi-parental RIL population, and (iii) validate the major QTL identified on chromosome five in the RIL population. Association mapping identified 12 significant markers that accounted for 27.2 percent and 8.9 percent of the phenotypic variation for IDC in the two populations, respectively. These markers co-localized with several known iron related QTL and genes. A significant cluster of 11 markers on chromosome five co-localized with the major IDC QTL identified in the bi-parental Fiskeby III X Mandarin (Ottawa) population. A second potential candidate gene was identified in this QTL region that may be related to IDC in soybean.

Table of Contents

List of Tables

Chapter 1

Chapter 2

List of Figures

Chapter 2

Chapter 3

Chapter 4

Chapter 1: Literature Review

Iron Deficiency Chlorosis

The soybean (*Glycine max* (L.) Merr.) has long been regarded as a culturally, and more recently, economically important crop since its domestication occurred in Northern China around the eleventh century B.C. (Gibson and Benson, 2005). It was not until the late eighteenth century that the soybean was first cultivated in the United States. Utilization of the soybean has come a long way since its application in medicine and as a staple food in China in 1100 B.C. Today, soybeans are used to produce an extensive array of end products including soybean meal and oil, margarine, salad dressing, tofu, paint, lecithin, printing inks, pharmaceuticals, and soy based biodiesel (Gibson and Benson, 2005). Due to the many applications of the soybean, it has become the second most valuable crop in terms of cash sales and the most valuable exported crop of the United States. In 2013, 31 million hectares of soybeans were planted and 89.5 million metric tons were harvested with a total crop value exceeding 41 billion dollars in the United States alone. This accounted for 32 percent of the world's total soybean production. The average price paid to farmers per metric ton of soybean in the U.S. was $478 in 2013, marking the second highest average price ever recorded (Soy Stats, 2014). With an increasing demand and rising commodity prices, emphasis must be put on research that may improve the overall production of the soybean crop worldwide.

Soybeans, like all crops, are subject to many different forms of abiotic stress. An especially important stress in the North Central United States is iron deficiency chlorosis (IDC). IDC occurs on calcareous soils and is a result of the inability of the soybean to utilize the form of iron that is present in the soil. Soybeans deficient in iron display the classic phenotype of interveinal chlorosis of young leaves, stunted growth, and

consequently, a reduction in yields. Economic losses stemming from yield reduction due to IDC are estimated at 260 million dollars per year (Peiffer et al., 2012). A survey completed in 2003 of soybean growers in western Minnesota noted that 99% of the farmers surveyed indicated that iron deficiency chlorosis was a major issue in their fields, affecting approximately 24% of their planted soybean hectarage (Hansen et al., 2003).

Physiological Mechanisms and Soil Properties Linked to Iron Deficiency Chlorosis

The soybean's physiological response to iron deficiency chlorosis and the associated soil chemical and physical properties are extremely complex, and therefore, have been researched extensively over the years. The research has been somewhat inconclusive in some aspects, partially due to the extremely variable nature of IDC across years and field locations that can be observed. However, there is a great deal of work with conclusions that are widely agreed upon which are presented below.

Inorganic iron in the form of Fe^{III+} is the predominant species found in calcareous soils, however, soybeans can only utilize the Fe^{II+} form so they must first reduce Fe^{III+} to Fe^{II+} before it can be taken up by the roots. Fe^{III+} solubility decreases a thousandfold for every one unit increase in pH above a pH of 4.0, so it becomes very difficult for soybeans to utilize the iron in the soil in highly calcareous soil conditions (Latimer, 1952). Plants have adopted different ways to mobilize iron found in the rhizosphere so they can utilize it in development. Depending on how this is achieved, plants can be categorized as utilizing strategy one techniques or strategy two techniques. Strategy two techniques are only utilized by grasses. This strategy consists of the release of phytosiderophores from the roots, which form a complex with Fe^{III+} in the soil, and the resulting iron-phytosiderophore complexes are then taken up by the roots. Soybeans have been

classified as using strategy one for iron acquisition (Marschner et al., 1986). Strategy one consists of several different components that allow the soybean to utilize iron in the soil, including the preferential uptake of Fe^{II+} following the reduction of Fe^{III+} at the root surface as described by Chaney et al. (1972), the secretion of H^+ from the roots to promote the reduction of Fe^{III+} to Fe^{II+} as described by Römheld et al. (1984), and the release of iron chelates or reducing compounds by the roots as described by Hether et al. (1984). The most common strategy one mechanism is the increased activity of a reductase that is bound to the plasma membrane. With increased activity, the reductase promotes the enhancement of Fe^{III+} reduction to Fe^{II+} while an analogous splitting of Fe^{III+} chelates occurs at the plasma membrane (Marschner et al., 1986). When H^+ is extruded by the roots, it leads to acidification of the rhizosphere and subsequently, an increase in iron uptake by the plant. This increase in iron uptake is a result of augmented reductase activity and iron solubility in the rhizosphere. Work with soybean and maize demonstrated that the rhizosphere pH was lower than that of the bulk soil under iron stress, and the apical root zone pH was always over one pH unit lower than the basal root zones (Römheld and Marschner, 1984). Lower pH values in the apical root zones were thought to be connected with heightened H^+ secretion during cell extension (Weisenseel et al., 1979). Earlier research showed that younger lateral soybean roots had a greater reducing capacity than older roots. This increased capacity was pinpointed to the protoxylem in the region of the root between root cell elongation and maturation (Ambler et al., 1970). Chelating and reducing compounds identified as phenolic-type can also enhance mobilization of iron in the rhizosphere under the acidic conditions caused by iron stress (Hether et al., 1984). All of these physiological mechanisms are preceded by

structural modification of the roots in highly iron efficient cultivars. Modifications include an increase in root hair formation, swelling of the roots, and the formation of transfer cells in the epidermis near the root tips that coincide with iron translocation (Kramer et al., 1980; Romheld and Marschner, 1981; Landsberg, 1982; Römheld et al., 1982).

However, when soybeans are grown on calcareous soil with high HCO_3^- concentrations, the protons that are extruded by the roots get buffered to an extent great enough that a pH gradient steep enough to stimulate reductase activity cannot be fashioned (Romheld, 1987). Iron efficient ('Lakota,' 'Hawkeye,' 'Chippewa-64,' and 'Hodgson') and iron inefficient ('Williams,' 'Hark,' 'Anoka,' and 'Wayne') soybean cultivars grown in nutrient solution containing 4 or 6 *u*M of FeEDDHA with five increasing increments of HCO_3^- regressed on chlorosis score demonstrated that soybean chlorosis severity increased with each increase of HCO_3^- in the nutrient solution, regardless of iron concentration or iron efficiency status. However, soybeans grown in nutrient solution containing 6 *u*M of FeEDDHA had lower chlorosis scores than those grown in solution containing 4 *u*M of FeEDDHA, and iron efficient cultivars had lower chlorosis scores than iron inefficient (Coulombe et al., 1984).

The reductants released from iron deficient 'Hawkeye' (HA, iron efficient) and PI-54619-5-1 (PI, iron inefficient) soybeans were characterized (Brown and Ambler, 1973). The reductants are thought to contain phenolic compounds that help keep iron in the usable ferrous ($Fe^{II+)}$ form. In tomato, the major component of the reductant was identified as caffeic acid (Olsen et al., 1982). It was shown that 'Hawkeye' soybeans

released more reductant from their roots than PI soybeans leading to an increase in the amount of ferric (Fe^{III+}) iron reduced to ferrous iron, and therefore, an increase in the overall concentration of ferrous iron in the nutrient solution. Although an increase of reductants and Fe^{II+} in the nutrient solution was seen during iron stress, there was not an increase in the uptake of iron by either soybean. Therefore, Brown and Ambler (1973) concluded that something other than the concentration of reductant in the nutrient solution must control the uptake of iron by the soybean. Prior research using HA and PI soybeans showed that iron deficient HA soybeans had a greater reducing capacity of Fe^{III+} and pH than iron deficient PI and iron sufficient HA and PI, and concomitantly the roots absorbed more iron. As iron chlorosis of the soybeans developed, they were able to absorb iron at a greater capacity, with the most noted increase being from the HA iron deficient plant (Brown, 1963). This demonstrated the relationship between the soybean's ability to reduce iron into a useable form, the capacity of its roots to absorb iron, and the plant's susceptibility or tolerance to IDC.

Experiments with sunflower roots demonstrated that the chelating agent ethylenediamine di (o-hydroxyphenylacetic acid), known as EDDHA, does not get taken up by the roots in equal quantities as the iron it chelates. Instead, the EDDHA remains in the nutrient solution, and the iron is released to the roots (Tiffin and Brown, 1959). Once Fe^{II+} is absorbed by the roots, it is reoxidized to Fe^{III+} before it reaches the metaxylem. The Fe^{III+} is then chelated by organic acids, particularly citrate, and travels via the xylem to growing parts of the plant (Brown and Ambler, 1974). Using HA and PI soybeans, Brown and Tiffin (1965) demonstrated that regardless of the iron stress level, there is a significant relationship between iron and citrate in the stem exudate. If transported iron

increased, citrate also increased, and if iron decreased, a paralleled decrease in citrate resulted. Upon reaching plant areas where the iron will be utilized, research has proposed that the Fe^{III+} must again be reduced to Fe^{II+} before the plant can use it. This reduction seems to be enhanced by several factors. When grown in conditions with more ultraviolet-blue light, there was an enhanced capability of the reduction of Fe^{III+}. Furthermore, this reduction capability was enhanced by the organic ions malate and citrate in the presence of light (Olsen et al., 1982).

Longnecker and Welch (1990) carried out experiments with iron efficient 'Hawkeye' (HA) soybean, iron inefficient PI-54619 (PI) soybean, and iron efficient IS-8001 (IS) sunflower to determine if IDC resistant plants accumulate pools of iron in their root apoplast that act as a buffer against chlorosis development. Young HA soybeans (8 days old) accumulated a much larger pool of apoplastic iron in their roots than the PI soybean and IS sunflower. It was concluded that the capability of HA soybean to accumulate a greater amount of iron in its root apoplast may be connected with its resistance to IDC. The authors speculated that under iron stress this pool of apoplastic iron may be more available in the short-term for the plant to utilize compared with iron that has already been incorporated into the plant's root-cell organelles or metabolites.

Iron efficient and iron inefficient plants respond to iron stress differently when grown on soil containing nitrate-N. Iron inefficient plants release large amounts of OH ions when grown with nitrate-N, which increases the soil pH and leads to chlorosis. They continue to release OH ions until the nitrate in the soil is depleted. Iron efficient plants, however, decrease their uptake of anions when grown on nitrate-N, which leads to a net

extrusion of H^+ ions and a consequent decrease in the pH (Egmond and Aktaş, 1977). Aktas and Egmond (1979) compared the iron efficient soybean cultivar 'Hawkeye' (HA) and the iron inefficient cultivar T-203 for their response to increasing levels of nitrate-N in the soil. At the lowest levels of nitrate, both HA and T-203 roots excreted similar amounts of H^+, but as the level of nitrate-N in the soil increased, T-203 roots began to excrete OH^- at levels up to seven times greater than HA roots. The T-203 soybeans were chlorotic throughout the experiment at high levels of nitrate while the HA soybeans showed no chlorotic symptoms. At the lowest level of nitrate, the T-203 soybeans did, however, overcome the iron deficiency symptoms once the nitrate in the soil was depleted. The authors concluded that as more nitrate is assimilated, more OH^- ions are produced and excreted by the roots leading to an increase in the alkalinity of the rhizosphere, and therefore, a decrease in the solubility of iron.

Nitrogenase activity and symbiotic nitrogen fixation also play a role in IDC. Gibson and Bergersen (1980) demonstrated that there is a correlation between symbiotic nitrogen fixation and the release of H^+ into the rhizosphere when legumes are infected with *Bradyrhizobium*. Biological nitrogen fixation carried out by several legumes and the iron deficiency response both cause chemical reductions within the root. These two processes interact to cause an enhanced iron stress response (Soerensen et al., 1988; Terry and Jolley, 1994). Several experiments have been carried out with soybean to investigate the role of nitrogenase and nitrogen fixing nodules on the plant's iron stress response (Soerensen et al., 1988; Terry et al., 1991; Terry and Jolley, 1994). All three of these studies concluded that nodules must be actively fixing nitrogen in order for the plant to exhibit an iron stress response.

Potassium deficiency in soils has also been linked to IDC. In a study using an iron efficient tomato and soybean, it was shown that in the absence of potassium in nutrient solution, the plants were unable to respond to iron stress (Jolley et al., 1988). Lack of potassium prevented the release of H^+ ions and reductants from the plant roots, which resulted in a decreased level of Fe^{III+} reduction. Sodium and rubidium were substituted for potassium in solution but no enhancement of H^+ release was seen. Therefore, Jolley et al. (1988) concluded that their results agreed with the idea of Landsberg (1982) that a plasmalemma-located ATPase stimulated by potassium controls the release of H^+ from the roots.

Genetic Control of Iron Deficiency Chlorosis in Soybean

The first experiment designed to characterize the genetic inheritance of IDC resistance in soybean was carried out by Weiss in 1943. Six iron inefficient soybean cultivars and four iron efficient cultivars were selected and crossed reciprocally in every possible combination. According to the segregation seen for resistance to IDC, it was concluded that iron efficiency was controlled by a single gene. The varieties that were iron inefficient were assumed to all carry two copies of the same recessive *fe* allele, while the iron efficient varieties carried the *Fe* allele that showed complete dominance (Weiss, 1943). Later work by Cianzio and Fehr (1980) produced similar results as Weiss (1943). However, the authors observed deviations from Mendelian inheritance patterns in some progeny, so they concluded that resistance was controlled by a single major gene along with modifier genes of small effect. Based on the results from this work, Prohaska and Fehr (1981) carried out a recurrent selection breeding program in order to develop a soybean variety with increased IDC resistance. A significant linear improvement in the

mean chlorosis score was seen after two cycles of recurrent selection, indicating that IDC resistance was due to additive gene action, instead of the single gene model previously reported. Additional work by Cianzio and Fehr (1982) confirmed a quantitative inheritance model for IDC resistance in another soybean population. Recent mapping work of iron deficiency chlorosis resistance supports the polygenic model, and many QTL (Table 1) have been identified that exemplify a large number of small effect loci control the IDC phenotype (Lin et al., 1997, 2000; Charlson et al., 2003, 2005; Wang et al., 2008; O'Rourke et al., 2009; Peiffer et al., 2012).

Drought

In addition to iron deficiency chlorosis, another yield limiting abiotic stress facing soybean is drought. Globally, drought is considered to be the most detrimental weather-related stress affecting soybean, and in the United States it is the principal factor limiting soybean yields. Yield reductions of 40% as a result of drought have been reported in soybean (Specht et al., 1999). Water deficit during flowering and pod fill lead to the greatest decrease in yield due to a significant increase in flower and pod abortion (Westgate and Peterson, 1993). Plants can respond to drought stress in several ways and have developed three main mechanisms to manage the stress including drought avoidance, drought escape, and drought tolerance (Turner et al., 2001). Drought avoidance allows the plant to maintain high turgor during water stress conditions. Avoidance is achieved through the development of vast root systems, which allow for the efficient absorption of water, and by a reduction in water loss as a result of reduced evapotranspiration. The second mechanism, drought escape, is the ability of the plant to complete its life cycle before serious drought stress occurs. This mechanism is utilized in

parts of the southern United States where early maturing soybeans are planted in March and April and allowed to reach maturity before potential drought occurs in July and August (Heatherly and Elmore, 2004). Drought tolerance, the final mechanism, allows the plant to maintain turgor and continue growing, without any major penalties, even under low water potential conditions. These three mechanisms can be achieved using several different physiological and biochemical strategies as discussed below.

Soybean Response Mechanisms Under Drought

Genetic variation exists for many traits that allow soybean to cope with drought stress. The development of a long taproot early in the growing season allows the plant to reach further into the soil where water may be more abundant later in the growing season (Taylor et al., 1978). Furthermore, dense, fibrous root systems aid in the uptake of water and nutrients, and strong correlations exist between the mass, length, and volume of roots and the soybean's ability to handle stress (Liu et al., 2005).

Nitrogen fixation in soybean is extremely sensitive to drought. Increased soil drying leads to an increase in ureides in soybean xylem sap, which is thought to result in the inhibition of nitrogen fixation (Sinclair and Serraj, 1995). In addition, a close relationship between leaf and nodule water potential has been observed (Durand et al., 1987). Under drought conditions, the authors observed a 70% decrease in nitrogenase activity, which was partially attributable to an increased resistance of oxygen diffusion to the bacteroid. A plant introduction, PI 416937, has been identified that maintains high nitrogenase activity even under drought, most likely due to its extensive fibrous rooting structure that allows more surface area for nodulation (Hudak and Patterson, 1995). This

PI may hold value for future breeding efforts.

In addition to the below ground changes that occur under drought stress, soybean utilizes several above ground mechanisms to tolerate water stress. Leaf pubescent density plays an important role in keeping the plant cool by increasing reflectance from the leaves. Soybean lines with dense pubescence tend to have increased rooting depth and density as well as an overall increase in vegetative vigor (Garay and Wilhelm, 1983). Dense pubescence can also augment photosynthesis by reducing radiation penetration into the canopy and by restricting water loss due to transpiration (Specht and Williams, 1985). However, although dense pubescence is beneficial under drought stress, under normal conditions the alleles controlling dense pubescence can lead to increased plant height and lodging, delayed maturity, and a reduction in yield (Specht et al., 1985).

Another common mechanism of plants undergoing drought stress is to regulate their stomata to limit stomatal conductance. Stomatal conductance plays a central role in leaf gas exchange and water vapor loss. In soybean, research has indicated that decreased stomatal conductance was highly correlated with severe plant water stress (Bennett et al., 1987). Under a moderate soil water deficit, soybean roots produce abscisic acid (ABA) that is carried through the xylem to the leaves where it signals the stomata to partially close (Liu et al., 2003). This early signaling from the roots prior to a decrease in leaf turgor allows for an increase in the soybean's water use efficiency. Low leaf epidermal conductance is also a desirable trait for drought tolerance. Plants that are native to arid environments tend to have a low level of leaf epidermal conductance (Riederer, 2001), and agricultural crops with low leaf epidermal conductance have a tendency to survive

longer under severe drought stress than plants with higher levels of leaf epidermal conductance (Sinclair and Ludlow, 1986). A significant negative correlation has also been reported between water use efficiency and low levels of leaf epidermal conductance in drought conditions, which provides further evidence of the utility of this characteristic in plants suffering from reduced water availability (Hufstetler et al., 2007).

A final mechanism involved in the soybean's response to drought is osmotic adjustment (OA). Osmotic adjustment can be defined as the lowering of the osmotic potential due to the net accumulation of solutes in response to water deficits (Zhang et al., 1999). OA is important under drought stress because it allows the plant to maintain cell turgor under reduced tissue water potential. As soil begins to dry out, OA has been attributed to allowing the plant to improve its root growth and water uptake, reduce flower abortion, delay leaf senescence, and maintain photosynthesis and stomatal conductance (Turner et al., 2001).

Tolerance to drought, like IDC, is an extremely complex trait that is controlled by many genes and different metabolic pathways. There is also a significant genotype by environment interaction effect that further complicates the discovery of the underlying genes and mechanisms that control drought tolerance (Carter Jr et al., 1999). Several QTL have been identified that correspond to drought tolerance (Mian et al., 1996, 1998; Specht et al., 2001; Bhatnagar et al., 2005; Monteros et al., 2006; Carpentieri-Pipolo et al., 2011), but further work needs to be done to validate these QTL and test their efficacy in elite backgrounds.

Breeding for tolerance to drought in soybean has historically progressed slowly due to three main reasons as explained by Carter Jr et al. (1999). Most importantly, breeding in a high yielding environment leads to larger gains and returns than breeding in a low yielding environment, such as one that is drought prone. The ability to identify soybean cultivars with the highest yield potential is critical to a breeding program. However, low yielding environments are not good candidates for the discernment of high and low yielding cultivars, thus breeders tend to do their testing under ideal environmental conditions with adequate water. Furthermore, early breeding efforts in soybean focused on disease resistance, shatter resistance, and other agronomic factors instead of tolerance to abiotic stresses such as drought. This resulted in a reduced genetic base for drought tolerance in soybean breeding programs. Lastly, Carter Jr et al. (1999) suggested that breeding for drought tolerance is risky and difficult in that the occurrence of drought is unpredictable. This makes it difficult to select for drought tolerance over many years because the selection environment can vary greatly from year to year. This results in unreliable data.

Despite these difficulties, progress has been made in the challenge to improve drought tolerance in soybean. Most breeding efforts have focused on soybeans that display slow canopy wilting, prolific rooting, sustained nitrogen fixation, and higher yields under drought conditions (Sloane et al., 1990; Hudak and Patterson, 1995; Sinclair et al., 2000; Paris, 2003). In addition, there has been demonstrated success in improving drought tolerance by overexpressing several drought related genes in transgenic soybean lines (de Ronde et al., 2004; Chen et al., 2007).

Table 1: Reported IDC QTL in soybean arranged by linkage group[1]

Linkage Group/ Chromosome #	Soybase QTL Designation	Parent 1	Parent 2	Reference
A1/5	Fe effic 5-1	Anoka	A7	Lin et al. 1997
A2/8	Fe effic 1-1[2]	A81356022	PI468916	Diers et al. 1992A
B1/11	Fe effic 9-1	Pride B216	A15	Lin et al. 2000B
B2/14	Fe effic 10-3	Anoka	A7	Lin et al. 2000B
	Fe effic 11-1	Pride B216	A15	Lin et al. 2000A
	Fe effic 3-1	Pride B216	A15	Lin et al. 1997
	Fe effic 3-2	Pride B216	A15	Lin et al. 1997
	Fe effic 4-1	Pride B216	A15	Lin et al. 1997
	Fe effic 8-1	Pride B216	A15	Lin et al. 1997
	Fe effic 9-2	Pride B216	A15	Lin et al. 2000B
D1a/1	Fe effic 1-2[2]	A81356022	PI468916	Diers et al. 1992A
	Fe effic 1-3[2]	A81356022	PI468916	Diers et al. 1992A
	Fe effic 1-4[2]	A81356022	PI468916	Diers et al. 1992A
G/18	Fe effic 1-5[2]	A81356022	PI468916	Diers et al. 1992A
	Fe effic 3-3	Pride B216	A15	Lin et al. 1997
	Fe effic 7-1	Pride B216	A15	Lin et al. 1997
	Fe effic 8-2	Pride B216	A15	Lin et al. 1997
	Fe effic 9-3	Pride B216	A15	Lin et al. 2000B
H/12	Fe effic 11-3	Pride B216	A15	Lin et al. 2000A
	Fe effic 8-3	Pride B216	A15	Lin et al. 1997
I/20	Fe effic 10-1	Anoka	A7	Lin et al. 2000B
	Fe effic 11-2	Pride B216	A15	Lin et al. 2000A
	Fe effic 12-1	Anoka	A7	Lin et al. 2000A
	Fe effic 4-2	Pride B216	A15	Lin et al. 1997
	Fe effic 6-1	Anoka	A7	Lin et al. 1997
L/19	Fe effic 9-4	Pride B216	A15	Lin et al. 2000B

[1] Table adapted from: http://www.soybase.org/search/index.php?qtl=Iron%20efficiency

[2] QTL in main population did not match QTL in tester set

Chapter 2: Iron Deficiency Chlorosis QTL Mapping and Characterization of the Fiskeby III X Mandarin (Ottawa) Recombinant Inbred Line Population

Introduction

With an increased variance in the weather and an ever-changing uncertainty about the climate, a better understanding of abiotic stresses that are affecting and may affect soybeans in the future is becoming more and more critical. Iron deficiency chlorosis expression is already extremely variable within and across environments and years, thus, any increased variation in weather patterns will most likely lead to an increased difficulty to predict chlorotic problems in the field. The current study evaluates a recombinant inbred line (RIL) soybean population for its phenotypic response to iron deficiency chlorosis (IDC). The RIL population was created by crossing the IDC tolerant Fiskeby III to the IDC susceptible Mandarin (Ottawa). Fiskeby III is very unique in that it has been shown to be tolerant to IDC, drought, ozone, salt, aluminum and cold weather (Holmberg, 1973; Burkey and Carter, 2009). Because of the extremely diverse pedigree of the Fiskeby III X Mandarin (Ottawa) population, along with Fiskeby III's rare tolerance to a multitude of abiotic stresses, the potential exists for the discovery of novel alleles that may provide soybean with abiotic stress tolerance that is missing in today's elite breeding material. This research and the collaborative research being carried out by the USDA will provide us with insights into the interactions between multiple abiotic stress responses as well as give breeders more potential tools to increase soybean tolerance to these stresses. The objectives of this chapter are to (i) characterize the Fiskeby III X Mandarin (Ottawa) RIL population for its tolerance to iron deficiency chlorosis; (ii) identify quantitative trait loci (QTL) via composite interval mapping for iron deficiency chlorosis in the RIL population; and (iii) identify co-localization of abiotic stress QTL and putative candidate genes for iron deficiency chlorosis tolerance.

Materials and Methods

Mapping Population Development

The iron-efficient soybean Fiskeby III (PI 438471, maturity group 000) was crossed to the iron-inefficient Mandarin (Ottawa) (PI 548379, maturity group 0) to create a $F_{5:6}$ population of 239 recombinant inbred lines. Sven Holmberg, a soybean breeder in Fiskeby, Sweden, developed Fiskeby III through the hybridization of Namikawa (Sachalin) and Typ xx stam 9 and released Fiskeby III in 1949 for use as an edamame soybean. Namikawa (Sachilin) originated from a Japanese island, most likely Hokkaido, where it was a landrace. The origin of Typ xx stam 9 is unknown, however, it was used in Europe as a breeding line. Mandarin (Ottawa) was selected from the Chinese landrace Mandarin for its early maturity in Ottawa, Ontario in 1934. Pedigree analysis (Gizlice et al., 1994) indicates that Fiskeby III only accounts for 0.5 percent of the genetic variation in North American lines. Mandarin (Ottawa) accounts for 12 percent of the genetic variation in North American lines and is a parent of 12 U.S. soybean cultivars.

The hybridization of Fiskeby III to Mandarin (Ottawa) took place in the USDA-ARS greenhouse in Raleigh, North Carolina in the Summer of 2006. F1 seed was harvested and planted in a winter nursery in Chile in 2006-2007. F2 seed was harvested and subject to inbreeding using the single seed descent method until the F5 generation (Brim, 1966). During single seed descent, plants were grown in Minnesota during the summers and in the winter nursery in Chile during the winter in 2007-2009. F5 seed was planted in the greenhouse at the USDA-ARS facility in Raleigh, North Carolina in the winter of 2010, individual F5 plants were harvested, and the seed was bulked. To ensure that segregation patterns were consistent with those expected using single seed descent,

the growth habit, pubescence color, and pod-wall color was recorded for each plant. The F5 derived bulked seed was then planted in the summer of 2010 in Minnesota in progeny rows. Resulting $F_{5:7}$ seed was harvested and bulked for use in this study.

Experimental Design

The 239 recombinant inbred lines (RILs) were planted in two ongoing iron chlorosis nurseries in Danvers and Madison, Minnesota in 2011, 2012, and 2013. The nurseries were located in a specific area of a farmer's field where iron chlorosis was a reoccurring problem. However, chlorotic symptoms did not appear in Madison in any of the three years, so data was only obtained from the Danvers location. In the 2011 field location in Danvers, soil types consisted of 50 percent Bearden-Quam (complex, fine-silty, mixed, superactive, frigid Cumulic Endoaquolls), 30 percent Byrne (fine-loamy, mixed, superactive, frigid Calcic Hapludolls), and 10 percent each of Quam (fine-silty, mixed, superactive, frigid Cumulic Endoaquolls) and Malachy (coarse-loamy, mixed, superactive, frigid Aquic Calciudolls). The 2012 field location consisted of 40 percent Bearden-Quam, 40 percent Rockwell (coarse-loamy, mixed, superactive, frigid Typic Calciaquolls), and 10 percent each of Quam and Hecla (sandy, mixed, frigid Oxyaquic Hapludolls). The 2013 field location consisted of 90 percent Bearden-Quam and 10 percent Quam. The pH of the soils throughout the field locations ranged from 7.8 to 8.4. All soil series shared the common characteristic of being poorly drained, depressional areas that tend to be prone to iron deficiency chlorosis symptoms.

A randomized complete block design was used when planting the RILs. Plots were planted on 3 June in 2011, 22 May in 2012, and 30 May in 2013. All plots had 75 centimeter row spacing, were 90 centimeters in length, and 25 seeds were planted per

plot. Each plot was replicated three times in 2011 and 2012 with chlorosis checks located within each 100-plot block. Only two replications were planted in 2013 due to a shortage of seed. Seven check lines were utilized each year in the field including Fiskeby III (RIL parent, resistant), Mandarin (Ottawa) (RIL parent, susceptible), 'MN0095' (resistant check), 'Sheyenne' (resistant check), 'Dawson' (resistant check), 'Corsoy 79' (susceptible check), 'Bicentennial' (susceptible check used in 2011), 'Parker' (susceptible check used in 2012), and 'Lambert' (susceptible check used in 2013). Iron chlorosis severity can vary greatly on a spatial scale throughout a field, so the checks allowed for standardization of the blocks if variation of chlorosis intensity was seen throughout the nursery.

Phenotypic Evaluation

Iron chlorosis was scored for each repetition at the V3 stage and again at the V6 stage using a 1-9 chlorosis severity rating scale on a whole-plant basis (Figure 1). A score of 1 indicated a healthy, green plant with no signs of chlorosis, and a score of 9 indicated a severely chlorotic and necrotic plant. In 2011, plants were scored on 5 July (V3) and 25 July (V6), in 2012, plants were scored on 28 June (V3) and 18 July (V6), and in 2013 plants were scored on 9 July (V3) and 23 July (V6). A handheld field computer was utilized to record all scores.

Genotypic Evaluation

Fiskeby III, Mandarin (Ottawa), and the 239 F5 derived RILs were planted in the USDA-ARS greenhouse in Raleigh, NC. Qiagin DNeasy Plant Mini Kits in a QiaCube workstation (Qiagin, Hilden, Germany) were utilized to extract DNA from 15-20 bulked

primary root tips for each RIL. DNA was sent to the USDA-ARS in Beltsville, Maryland to be genotyped. One thousand five hundred thirty-six single nucleotide polymorphism (SNP) markers were genotyped using the Illumina GoldenGate assay, and analysis was completed following the protocol described by Fan et al. (2006) on the Illumina *BeadStation 500G* (Illumina Inc, San Diego, CA). Illumina's *Genome Studio* software (version 2011.1) was used to manually check each allele call. The following criteria were used to exclude markers that did not satisfy these conditions: call frequency (<95%), GenTrain score (<0.25), cluster separation (<0.20) with ABT Mean (<0.20 or 0.80-1.00), or monomorphism (100% AA or BB). The software package *R*/*qtl* (R Development Core Team, 2012) was used to evaluate the quality of the linkage map by checking for duplicate and missing markers, marker order compared to the USDA consensus map (Hyten et al., 2010), similar individuals, and segregation distortion. Upon completion of marker allele calls and map quality evaluation, 366 SNP markers were retained for quantitative trait loci (QTL) analysis. The final map length was 1811 cM with an average marker spacing of 5.2 cM (Table 2).

Statistical Analysis

R Studio, version 0.97.449 (R Development Core Team, 2012) was utilized to carry out statistical analyses. An overall average score was calculated for each RIL by taking the average of the three repetitions (two in 2013) over the two scoring dates in each year. Results from an analysis of variance (ANOVA) were used to calculate the narrow sense heritability on an entry mean basis. The following equation was used to calculate heritability:

$$h^2 = \sigma_G^2 / [(\sigma_e^2 / ry) + (\sigma_{GY}^2 / y) + (\sigma_G^2)]$$

h^2 is the narrow sense heritability on an entry mean basis

σ_G^2 is the genetic variance

σ_e^2 is the error variance

σ_{GY}^2 is the variance of the genotype by year interaction

r is the number of repetitions

y is the number of years

Due to the extremely variable nature of iron chlorosis symptoms throughout a field, two different score adjustment procedures were compared for their effectiveness to account for any variation that was present. First, average IDC scores from scoring dates one and two were used to calculate genotypic least square means (LS-means) for each repetition of the RILs. A restricted maximum likelihood (REML) approach in R was used to calculate the LS-means and estimate variance components. The following mixed model was used to calculate LS-means for the RILs across and within years. Replications, years, and genotypes were treated as random variables.

$$Y_{jkm} = \mu + R(E)_{k(j)} + E_j + G_m + GE_{mj} + e_{jkm}$$

Y_{jkm} is the iron chlorosis score in the jth year, kth replication, and mth genotype

μ is the overall mean iron chlorosis score

$R(E)_{k(j)}$ is the random effect of the kth replication nested in the jth year

E_j is the random effect of the jth year

G_m is the random effect of the mth genotype

GE_{mj} is the interaction of the mth genotype and jth year

e_{jkm} is the random error associated with the jth year, kth replication, and mth genotype

Least square means of each repetition were averaged to get final LS-mean IDC scores for each RIL.

The second score adjustment procedure was carried out in GenStat version 16 (VSN International, 2014) using the spatial analysis and correlation modeling packages. GenStat utilizes a mixed correlation model with values in the correlation matrix **C** defined using the auto-regressive order 1 (AR1). AR1 is defined by: $c_{i+k,i} = \phi^k$, $c_{i,i} = 1$ where c is the correlation between two plots, k is the distance between plots, and ϕ is a correlation constant. For the spatial model, a correlation model is fitted to a random term where the factors in the random term represent row and column positions throughout the field. A separable correlation model is then fitted, in which the correlation between the plots at coordinates (i,j) and (k,l) is the product of a correlation from a model defined on the rows of the field, and a correlation from a model defined on the columns of the field. This can be visualized as: correlation cr_{ik} between rows $(i\text{-}k)$ apart * correlation cc_{jl} between columns $(j\text{-}l)$ apart where the correlations cr_{ik} and cc_{jl} are defined by AR1 (Payne et al., 2011).

Raw average, LS-mean, and GenStat adjusted IDC scores were checked for normality using Q-Q plots and tests of skewness and kurtosis in R. Q-Q plots indicated normality for all data and skewness and kurtosis was minimal, therefore, no further data transformations were necessary.

Quantitative Trait Loci (QTL) Mapping

Composite interval mapping (CIM) in the R/qtl (Broman et al., 2003) statistical package was utilized to map quantitative trait loci (QTL) in the bi-parental Fiskeby III X Mandarin (Ottawa) population. The "cim" function in R/qtl uses a scheme from QTL Cartographer in which forward selection is first done at the markers, and then interval mapping is carried out with the selected markers as covariates. Selected marker covariates are dropped if they are located within a fixed window size of the position being tested (Broman et al., 2003). Composite interval mapping was performed using five marker covariates, a window size of 10 cM, and a walking speed of 2 cM. 1000 permutation tests were conducted using a genome-wide significance level of 0.05 in order to determine the likelihood of odds (LOD) threshold for declaring QTL significance (Doerge and Churchill, 1996). Haley-Knott regression was utilized to determine the amount of phenotypic variation significant QTL accounted for, as well as marker effect size on the 1-9 phenotypic rating scale.

Separate analyses were conducted using the raw average, LS-mean, and GenStat adjusted IDC scores. Mapping was carried out using an overall phenotypic mean from 2011, 2012, and 2013. In addition, each year was analyzed separately using the three different score adjustment methods to further validate significant QTL.

Results and Discussion

Phenotypic Characterization

Significant differences in IDC scores were seen between the RILs over the three years (Table 3). The mean IDC score was 3.92, 2.94, and 5.69 in 2011, 2012, and 2013 respectively. The overall average IDC score was 4.18 for all the RILs. Scores in all three

years followed a normal distribution (Figures 2,3,4,5), indicating that resistance to chlorosis in this population is quantitatively inherited as has been seen in most populations studied for IDC (Rodriquez de Cianzio and Fehr, 1982; Lin et al., 1997; Charlson et al., 2005). Differences in means between the iron efficient parent, Fiskeby III, and the iron-inefficient parent, Mandarin (Ottawa), were also significant for each of the three years (Table 3). The average IDC score for Fiskeby III and Mandarin (Ottawa) over three years was 3.25 and 5.19, respectively. Fiskeby III had a lower IDC score on average than Mandarin (Ottawa) in all three years, indicating the consistency of Fiskeby III's resistance and Mandarin (Ottawa's) susceptibility throughout multiple environmental conditions. This confirms what was previously observed for Fiskeby III and Mandarin (Ottawa) and exemplifies the efficacy of utilizing these two cultivars for the RIL population development. Average IDC scores were significantly higher in 2013 than in 2011 and 2012. This can most likely be attributed to the extremely wet spring in 2013. Wet field conditions in the early part of the growing season cause CO_2 to dissolve to form carbonic acid, which leads to HCO_3^- in equilibrium concentrations (Lucena, 2000). This increase in HCO_3^- concentration further exacerbates chlorotic symptoms.

Results from the ANOVA analyzing the 2011, 2012, and 2013 data together indicated that there was a highly significant ($p<0.001$) effect on IDC due to year, genotype, and genotype by year interaction (Table 4). The interaction of repetition by year was less significant ($p<0.1$), and the effect of repetition was not significant. Analyzing each year separately indicated that the effect of genotype was highly significant in 2011 and 2012, but the effect of repetition was not significant (Tables 5 and 6). In 2013, the effect of genotype and repetition was significant (Table 7). It is

somewhat surprising, but not unexpected, that no significant effect due to repetition was seen in 2011 or 2012 due to the extremely variable nature of chlorotic symptoms that can be seen across a field. The plots in 2011 and 2012 were located in a small area in the basin of a depressional area of the field where consistent IDC symptoms had been seen in the past. The consistency of soil type and moisture in this depressional area most likely lead to a non-significant repetition effect. However, in 2013 the two repetitions were significantly different in their IDC scores. This was expected since the first repetition was planted in the basin and on the rim of a depressional area, while the second repetition was planted above the depressional area. Previous research has shown that chlorosis symptoms are more severe around rims of depressional areas because insoluble salts and mobile ions that correlate with IDC tend to accumulate on these rims (Inskeep and Bloom, 1984). This difference in field topography most likely accounted for the variation seen between repetitions in 2013.

Although no significant effects were seen due to repetitions in the combined three year data, the two score adjustment procedures were still utilized to potentially correct for any within repetition variation that was present. No significant differences were seen in any of the three years between the means for the raw average, LS-mean, or GenStat adjusted IDC scores (Table 8). However, there was a significant decrease in the standard deviation and the range of the LS-mean scores compared to the raw average and GenStat adjusted scores. Standard deviations and ranges of scores were not significantly different between raw average and GenStat adjusted scores. It was not surprising that significant differences were not seen between the adjusted data and the raw data means upon analyzing the three years with an ANOVA. Although the effect due to repetition in 2013

was significant, the lack of variation in 2011 and 2012 acted as a buffer when all three years of data were combined, which resulted in a non-significant repetition effect across the three years. The goal of least square means is to minimize the sum of squared residuals in the model, thus reducing the amount of error variance. This can explain why there were significantly lower standard deviations in the GenStat adjusted data compared to the raw and LS-mean data. Also, the LS-mean procedure tended to shift high and low values closer to the mean, which resulted in smoother data and a smaller range of scores.

The heritability on an entry mean basis was 0.61 for IDC over the three years evaluated. This was very similar to the heritability observed in several other IDC studies (Lin et al., 1997, 2000; Charlson et al., 2005), and confirmed the consistency of our scoring over the three years. Variance components estimated via REML are represented as a percentage of the total variation (Table 9). The percentage of variation attributable to years was the highest out of all factors at 54 percent. Genotypes accounted for 9.8 percent of the variation while genotypes nested within years accounted for 9.6 percent of the variation. The variance of repetitions and repetitions nested within years was negligible. Error variance accounted for 26.4 percent of the total variation. The fact that years accounted for over half of the variation is not surprising. Growing seasons differed dramatically across the three years and plots were planted in different locations in an 80-acre field each year. 2012 marked one of the warmest and driest springs in recent history, while 2013 was cool and wet for most of the early part of the growing season. The effects that these significant differences in growing conditions had on IDC scores can be easily seen in the average scores between the years and can also explain the large variance attributable to years. Surprisingly, the error variance was low for an iron

chlorosis study. Another recent QTL mapping project for IDC resistance reported an error variance of 40-78% depending on the population (Jones, 2013). The low error variance in this study may be explained by the use of a single scorer for the IDC plots over the course of the three years as well as the consistency of soil properties within the IDC nursery locations. Error variance most likely would have been reduced further if the Madison, MN nursery location would have exhibited chlorotic symptoms. This would have provided us with three more years of data with three repetitions each year. Since chlorosis symptoms can vary greatly between years and locations, this additional site would have resulted in more power to minimize the error variance.

Composite Interval Mapping of Iron Deficiency Chlorosis

Quantitative trait loci significantly associated with iron deficiency chlorosis were detected using all three score adjustment procedures. The same two markers, 044481-08709 located on chromosome five and 014557-01578 located on chromosome six, were consistently detected using raw average, LS-mean, and GenStat adjusted mean IDC scores (Figure 8). The QTL detected using raw average IDC scores on chromosome 5 had a peak LOD position at 22 cM with a LOD score of 11.2. The 1.5-LOD support interval spanned from 18-24 cM while the Bayesian credible interval spanned a more narrow 20-22 cM interval (Table 10). This QTL explained 17.3 percent of the phenotypic variation for IDC and caused a 0.32 decrease in the IDC score per allele copy at this marker locus. Therefore, plants with this marker allele had an IDC score that was 0.64 lower on average than plants without this marker allele due to the fact that the RILs were essentially homozygous at all analyzed marker loci (Figure 6). The QTL detected on chromosome 6 had a peak LOD position at 67 cM with a LOD score of 5.4. The 1.5-

LOD support interval spanned from 51-89 cM while the Bayesian credible interval spanned a 55-83 cM interval (Table 10). This QTL explained 7.5 percent of the phenotypic variation for IDC and caused a 0.20 decrease in the IDC score per allele copy at this marker locus (Figure 7). Both marker alleles that caused a decrease in IDC scores among RILs came from Fiskeby III's genetic background.

The QTL detected using LS-mean IDC scores on chromosome 5 had a peak LOD position at 22 cM with a LOD score of 8.8. The 1.5-LOD support interval spanned from 18-24 cM while the Bayesian credible interval spanned a 20-22 cM interval. This QTL explained 16.2 percent of the phenotypic variation for IDC and caused a 0.25 decrease in the IDC score per allele copy at this marker locus (Table 11). The QTL detected on chromosome 6 had a peak LOD position at 67 cM with a LOD score of 4.8. The 1.5-LOD support interval spanned from 51-87 cM while the Bayesian credible interval spanned a 57-81 cM interval. This QTL explained 7.7 percent of the phenotypic variation for IDC and caused a 0.16 decrease in the IDC score per allele copy at this marker locus (Table 11).

The QTL detected using GenStat adjusted IDC scores on chromosome 5 had a peak LOD position at 22 cM with a LOD score of 8.5. The 1.5-LOD support interval spanned from 18-24 cM while the Bayesian credible interval spanned a 20-22 cM interval. This QTL explained 14.0 percent of the phenotypic variation for IDC and caused a 0.27 decrease in the IDC score per allele copy at this marker locus (Table 12). The QTL detected on chromosome 6 had a peak LOD position at 67 cM with a LOD score of 5.5. The 1.5-LOD support interval spanned from 55-89 cM while the Bayesian credible interval spanned a 59-83 cM interval. This QTL explained 8.5 percent of the

phenotypic variation for IDC and caused a 0.20 decrease in the IDC score per allele copy at this marker locus (Table 12).

It is important to note that although no significant differences were observed between the phenotypic means of the raw, LS-mean, or GenStat adjusted IDC scores, there was a slight difference between the percent variation explained by the QTLs each method detected. For example, when using the raw average scores compared to the LS-mean scores, a 1.1% increase in the percent variation explained by the QTL on chromosome five was observed. Although this difference was not significant, the variation explained by this QTL using the raw average scores was likely slightly overestimated. The raw average scores did not take into account any spatial variation across the field besides averaging the three repetitions, therefore, the LS-mean and GenStat adjusted estimate represented a more conservative estimate of the percent of variation explained. However, since all methods yielded similar results for how much variation the two identified QTL accounted for, I am confident that an average of the estimates is accurate.

Identification of Potential Candidate Genes

The QTL identified on chromosome five that was associated with marker 044481-08709 warrants further discussion due to its highly significant nature and the large amount of phenotypic variation it explained for IDC. Until very recently, there had only been one other QTL identified on chromosome five associated with IDC (Lin et al., 1997, 2000), however, this QTL was located much further downstream on the consensus map at 110 cM, which suggests that the QTL identified in the current experiment is different. Due to the relatively narrow confidence interval for this QTL region, SoyBase's genome

browser (http://soybase.org/gb2/gbrowse/gmax1.01/ [accessed 24 July 2014]) was utilized to search for possible candidate genes in the region. A candidate gene (Glyma05g09390) was identified that contained the SNP marker that was significantly associated with IDC in this study (Table 13). Glyma05g09390 is a gene that codes for the iron-containing enzyme, ferredoxin/thioredoxin reductase (FTR). Thioredoxins are known to regulate a vast number of enzymes that are directly involved in several varying chloroplast processes through redox mechanisms, thus any interruption in the FTR system would likely lead to pleiotropic effects on plant physiology (Balmer et al., 2003). In *Arabidopsis*, plants with a mutation in the variable subunit of FTR exhibited chlorotic symptoms under unfavorable culture conditions (Keryer et al., 2004). The authors concluded that the mutation in FTR lead to an extremely low endogenous activation rate of NADP-malate dehydrogenase (NADP-MDH). NADP-MDH is thought to have an antioxidant effect in the chloroplast compartment in C3 plants that prevents over-reduction of the electron transport chain constituents and consequent photoinhibition (Scheibe, 1987). Therefore, the inability of NADP-MDH to be properly activated in the FTR mutants could be leading to the loss of plant's ability to cope with certain oxidative stress, and thus the chlorotic phenotype.

These prior results in *Arabidopsis* led to the hypothesis that there may be a mutation in the FTR gene in the IDC susceptible Mandarin (Ottawa) parent that is resulting in the same chlorotic phenotype as seen in the *Arabidopsis* FTR mutants. For this reason, we decided to sequence Glyma05g09390 in both Fiskeby III and Mandarin (Ottawa) to see if there were any sequence differences. Sequence results indicated that there were two SNPs located within the gene, with one of the SNPs causing a substitution

of Alanine to Valine in the coding region. However, this substitution was caused by the SNP in the original sequencing panel, and therefore, cannot confirm the potential of Glyma05g09390 being the causative gene. Additionally, both Fiskeby III and Mandarin (Ottawa) were analyzed for copy number variation of Glyma05g09390, but both lines had a single copy of the gene. In order to further investigate the potential role that Glyma05g09390 plays in the soybean IDC response, sequencing of the gene in hundreds of different soybean lines should be carried out so the frequency of the Valine haplotype could be ascertained. If this haplotype is found to be rare, it could be hypothesized that this is a novel source of IDC resistance.

In a recently published association mapping study for IDC, a QTL was identified that localized to the same interval as the QTL found on chromosome five in the present study (Mamidi et al., 2014). The authors identified two additional potential iron related candidate genes separate from the candidate gene identified in the current study. The first gene was an Argonaute (AGO) like protein that was predicted to have a role in the soybean's stress response, and the second gene was a RAS-related nuclear protein that has been shown to be involved in copper trafficking and iron transport (Woeste and Kieber, 2000; Vaucheret, 2008; Mamidi et al., 2014). Identification of this QTL in an association mapping panel exemplifies that it is not population specific, which gives further credibility to its use for marker-assisted selection to improve IDC tolerance in soybean.

The significant marker associated with the smaller effect QTL identified on chromosome six was found to be located adjacent to a known iron associated gene, Glyma0614450 (Table 13). Glyma0614450 is an ATP-binding cassette transporter that is

a member of the ABC transporter superfamily. Proteins in this superfamily mediate the transport of a wide range of molecules across membranes, mostly against concentration gradients (Higgins, 1992). A mutant study that investigated Glyma0614450's homolog in *Arabidopsis,* ATM3, found mutant plants that expressed chlorotic and stunted phenotypes (Kushnir et al., 2001). The authors suggest that this phenotype is stress related and arises as a secondary effect due to a misbalance of intracellular iron homeostasis. In a second mutational study involving the ATM3 gene, authors observed mutant plants with reduced chlorophyll content and defects in root growth and seedling establishment (Bernard et al., 2009). They suggest that ATM3 plays a vital role in the biosynthesis of iron-sulfur complex proteins, which allows the chloroplasts to operate at their full photosynthetic capacity. These results suggest that Glyma0614450 may have a similar function in soybean that could play a role in the chlorotic response. Indeed, a recent genome-wide association study in soybean identified several significant markers adjacent to Glyma0614450 in one of the years of the study (Mamidi et al., 2011). In addition, expression data indicates that Glyma0614450 is almost exclusively expressed in the roots (Table 14). This further validates the potential of Glyma0614450 to be a candidate gene that may be a factor in the soybean's response to iron stress.

Conclusions

Significant differences were seen between the average IDC scores of the RILs across the three years. The extremely variable weather during the three years most likely accounted for these differences. Fiskeby III consistently scored significantly lower on average than Mandarin (Ottawa) in all three years for IDC severity. Average IDC scores of the RILs followed a normal distribution, indicating quantitative inheritance of IDC

tolerance in this population. An ANOVA indicated a significant effect due to year, genotype, and genotype by year interaction. The effect of repetitions was significant in 2013 but not in 2011 or 2012. The non-significant effect can be attributed to the consistency of field conditions across repetitions in 2011 and 2012 compared to 2013. Estimation of variance components via REML exemplified that years accounted for the most variation, followed by error and genotypes.

No significant differences were seen in any of the three years between the means for the raw average, LS-mean, or GenStat adjusted IDC scores. However, there was a significant decrease in the standard deviation and the range of the LS-mean scores compared to the raw average and GenStat adjusted scores. The non-significant effect of repetitions across the three years can explain why no significant difference was seen between the three score adjustment procedures. The error variance in this study was much lower than the error variance observed in another IDC study (Jones, 2013), which confirms the consistency of our scoring procedure and soil properties in the field. A further reduction in error variance may have been achieved if data from the Madison, MN location could have been obtained.

The same two markers were identified and found to be significantly associated with IDC among the three score adjustment procedures. A major QTL was identified on chromosome five and a minor QTL was detected on chromosome six that together accounted for approximately 25 percent of the phenotypic variation for IDC. Although no significant differences were seen between the results from the different score adjustment procedures, it is recommended to use one of the adjustment methods instead of just raw average scores for mapping. The non-significant repetition effect in this study

most likely is not normal for IDC, thus using a score adjustment procedure to account for in field variation should yield more accurate average IDC scores, and thus, more accurate mapping results.

Two potential candidate genes were identified as a result of the QTL mapping that may be important in soybean's response to IDC. Both genes have been shown to be important iron related genes in *Arabidopsis* (Kushnir et al., 2001; Keryer et al., 2004; Bernard et al., 2009), and mutations in these genes lead to similar phenotypes of the mutant *Arabidopsis* plants that are seen in iron deficient soybeans. However, further research needs to be carried out to determine the potential effectiveness of utilizing any of the identified markers for marker-assisted selection.

Table 2: Summary of the genetic map in the soybean recombinant inbred population Fiskeby III X Mandarin (Ottawa). Units used for measurement are reported in centimorgans (cM).

Chromosome	# of Markers	Length (cM)	AVG spacing (cM)	MAX spacing (cM)
1	14	76	5.8	19
2	23	126	5.7	22
3	24	90	3.9	22
4	24	67	2.9	44
5	18	84	4.9	18
6	16	130	8.7	31
7	17	59	3.7	22
8	18	115	6.8	16
9	18	86	5.1	17
10	17	116	7.3	35
11	7	94	15.7	35
12	18	82	4.8	46
13	34	92	2.8	15
14	17	85	5.3	20
15	26	81	3.2	20
16	25	74	3.1	12
17	7	59	9.8	17
18	16	95	6.3	36
19	12	100	9.1	49
20	15	100	7.1	36
Overall	366	1811	5.2	49

Table 3: Summary of iron deficiency chlorosis scores for the iron efficient Fiskeby III, the iron-inefficient Mandarin (Ottawa), and the recombinant inbred line population across three years. Scores represent an average of three repetitions in 2011 and 2012 and two repetitions in 2013 taken on a 1-9 chlorosis severity scale.

Genotype	Year			
	2011	2012	2013	Average
Fiskeby III	2.97**	1.43**	5.35*	3.25**
Mandarin (Ottawa)	5.37**	3.77**	6.45*	5.19**
RILs	3.92	2.94	5.69	4.18

**,* indicates significance at $p<0.01$ and $p<0.05$, respectively between Fiskeby III and Mandarin (Ottawa) within each year.

Table 4: Analysis of variance for iron deficiency chlorosis across 2011, 2012, and 2013.

Source	Df	Sum Sq	Mean Sq	F value	Pr(>F)
Year	2	2180.48	1090.24	1142.6490	< 2e-16 ***
Genotype	238	1120.27	4.71	4.9333	< 2e-16 ***
Rep	1	0.57	0.57	0.5969	0.43990
Year:Rep	2	4.81	2.41	2.5207	0.08083 ^
Year:Genotype	476	876.59	1.84	1.9301	< 2e-16 ***
Residuals	1192	1137.33	0.95		

***,^ indicates significance at the 0.001 and 0.1 probability levels, respectively.

Table 5: Analysis of variance for iron deficiency chlorosis in 2011.

Source	Df	Sum Sq	Mean Sq	F value	Pr(>F)
Genotype	238	614.12	2.58033	3.0555	< 2e-16 ***
Rep	2	0.02	0.01883	0.0223	0.8814
Residuals	476	402.81	0.84447		

*** indicates significance at the 0.001 probability level.

Table 6: Analysis of variance for iron deficiency chlorosis in 2012.

Source	Df	Sum Sq	Mean Sq	F value	Pr(>F)
Genotype	238	862.92	3.6257	2.9733	< 2e-16 ***
Rep	2	0.02	0.02	0.0182	0.8928
Residuals	476	580.44	1.2194		

*** indicates significance at the 0.001 probability level.

Table 7: Analysis of variance for iron deficiency chlorosis in 2013.

Source	Df	Sum Sq	Mean Sq	F value	Pr(>F)
Genotype	238	518.97	2.1806	3.3691	< 2e-16 ***
Rep	1	5.34	5.3353	8.2433	0.004459 **
Residuals	238	154.04	0.6472		

***,** indicates significance at the 0.001 and 0.01 probability levels, respectively.

Table 8: Summary of descriptive statistics for iron deficiency chlorosis for the three different score adjustment procedures.

Trait	Year	Mean	SD[1]	Median	Minimum	Maximum	Skewness	Kurtosis
IDC-R*	2011	3.92	1.18	4	1.5	7.5	0.4	-0.37
IDC-R	2012	2.94	1.45	3	0	8	0.47	-0.1
IDC-R	2013	5.69	1.19	5.5	2.5	8.5	-0.07	-0.64
IDC-R	11/12/13	4.18	1.71	4	0	8.5	0.06	-0.63
IDC-L**	2011	3.88	0.66	3.84	2.3	5.78	0.27	-0.08
IDC-L	2012	2.95	0.77	2.88	1.29	4.97	0.3	-0.58
IDC-L	2013	5.69	0.66	5.67	4.01	7.15	0.02	-0.72
IDC-L	11/12/13	3.98	1.28	3.84	1.29	7.15	0.35	-0.62
IDC-G***	2011	4.03	1.23	3.88	0	8.5	0.57	0.86
IDC-G	2012	2.79	1.76	2.67	0	8.39	0.23	-0.57
IDC-G	2013	5.43	1.02	5.39	2.24	9	0.34	0.45
IDC-G	11/12/13	3.88	1.77	3.97	0	9	-0.23	-0.26

* indicates raw average IDC score
** indicates LS-mean IDC score
*** indicates GenStat adjusted IDC score
[1] indicates standard deviation

Table 9: Variance components estimated via REML for iron deficiency chlorosis across 2011, 2012, and 2013.

Variance Component	Standard Deviation	Variance	Percent of Total Variance (%)
Genotype	0.5917	0.3501	9.8
Year	1.391	1.934	54
Rep	0.0640	0.0041	0.11
Genotype:Year	0.5861	0.3435	9.6
Rep:Year	0.0734	0.0054	0.14
Error	0.9718	0.9443	26.4

Table 10: Summary of results for composite interval mapping of iron deficiency chlorosis using raw average IDC scores. R^2 indicates the percent variation explained by the QTL. The sign of the additive effect refers to the Fiskeby III parent, where a positive additive effect indicates the Fiskeby III allele increases the IDC score, and a negative additive effect indicates the Fiskeby III allele decreases the IDC score. The additive effect represents the effect of a single "A" or "B" allele.

Trait	Marker	Chr	LOD Peak Position (cM)	LOD Score	1.5-LOD Support Interval (cM)	Bayesian Credible Interval (cM)	R^2 (%)	Additive Effect
IDC	044481-08709	5	22	11.2	18-24	20-22	17.3	-0.32
IDC	014557-01578	6	67	5.4	51-89	55-83	7.5	-0.20

Table 11: Summary of results for composite interval mapping of iron deficiency chlorosis using LS-mean IDC scores. R^2 indicates the percent variation explained by the QTL. The sign of the additive effect refers to the Fiskeby III parent, where a positive additive effect indicates the Fiskeby III allele increases the IDC score, and a negative additive effect indicates the Fiskeby III allele decreases the IDC score. The additive effect represents the effect of a single "A" or "B" allele.

Trait	Marker	Chr	LOD Peak Position (cM)	LOD Score	1.5-LOD Support Interval (cM)	Bayesian Credible Interval (cM)	R^2 (%)	Additive Effect
IDC	044481-08709	5	22	8.8	18-24	20-22	16.2	-0.25
IDC	014557-01578	6	67	4.8	51-87	57-81	7.7	-0.16

Table 12: Summary of results for composite interval mapping of iron deficiency chlorosis using GenStat adjusted IDC scores. R^2 indicates the percent variation explained by the QTL. The sign of the additive effect refers to the Fiskeby III parent, where a positive additive effect indicates the Fiskeby III allele increases the IDC score, and a negative additive effect indicates the Fiskeby III allele decreases the IDC score. The additive effect represents the effect of a single "A" or "B" allele.

Trait	Marker	Chr	LOD Peak Position (cM)	LOD Score	1.5-LOD Support Interval (cM)	Bayesian Credible Interval (cM)	R^2 (%)	Additive Effect
IDC	044481-08709	5	22	8.5	18-24	20-22	14.0	-0.27
IDC	014557-01578	6	67	5.5	55-89	59-83	8.5	-0.20

Table 13: Summary of three identified iron deficiency chlorosis candidate genes including their tentative annotation, chromosome location, and genomic position.

Gene	Annotation	Chromosome	Genomic Position
Glyma 05g09390	Ferredoxin/Thioredoxin reductase subunit A	5	9096700-9097908
Glyma 05g09210	MATE efflux family protein	5	8984514-8987590
Glyma 06g14450	ATP-Binding Cassette Transporter	6	11348069-11356906

Table 14: RNA sequencing read counts for three identified iron deficiency chlorosis candidate genes. “DAF” signifies days after flowering.

Gene	Young Leaf	Flower	One cm pod	Pod shell 10DAF	Pod shell 14DAF	Seed 10DAF	Seed 14DAF	Seed 21DAF	Seed 25DAF	Seed 28DAF	Seed 35DAF	Seed 42DAF	Root	Nodule
Glyma05g09390	49	34	37	29	29	4	11	12	25	20	27	21	19	26
Glyma05g09210	1	0	0	0	0	0	0	0	0	0	1	0	14	1
Glyma06g14450	0	0	0	0	0	0	0	1	0	0	1	0	18	0

Figure 1: Iron deficiency chlorosis severity rating scale utilized to collect phenotypic data. A score of one signified a healthy, green plant, while a score of nine signified an extremely stunted, chlorotic, and necrotic plant.

Figure 2: Distribution of iron deficiency chlorosis scores in 2011 with normality curve plotted. Scores represent an average of three repetitions taken on a 1-9 scale.

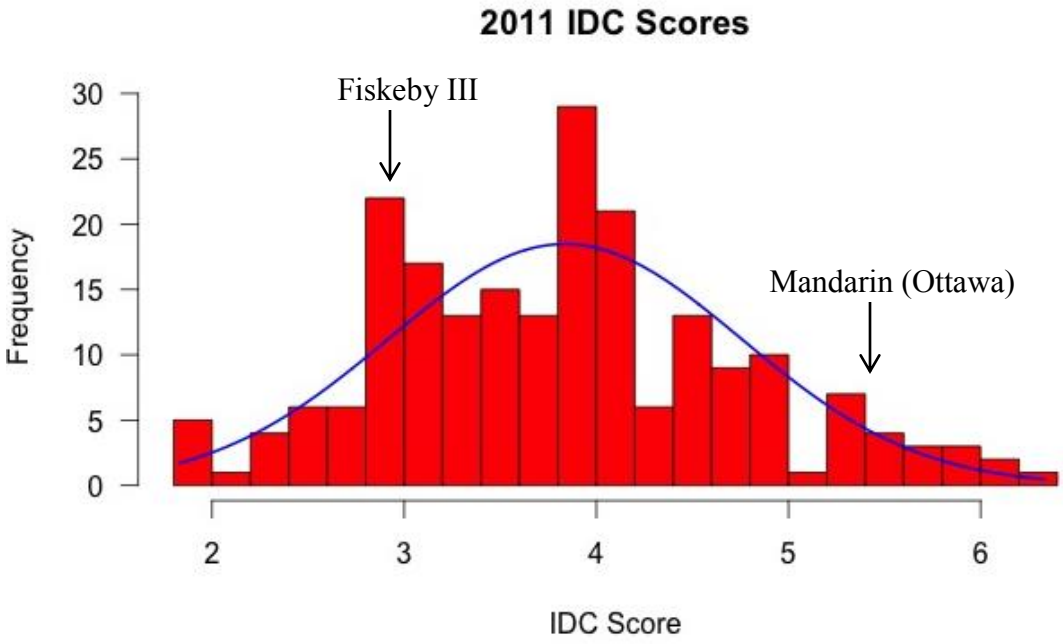

Figure 3: Distribution of iron deficiency chlorosis scores in 2012 with normality curve plotted. Scores represent an average of three repetitions taken on a 1-9 scale.

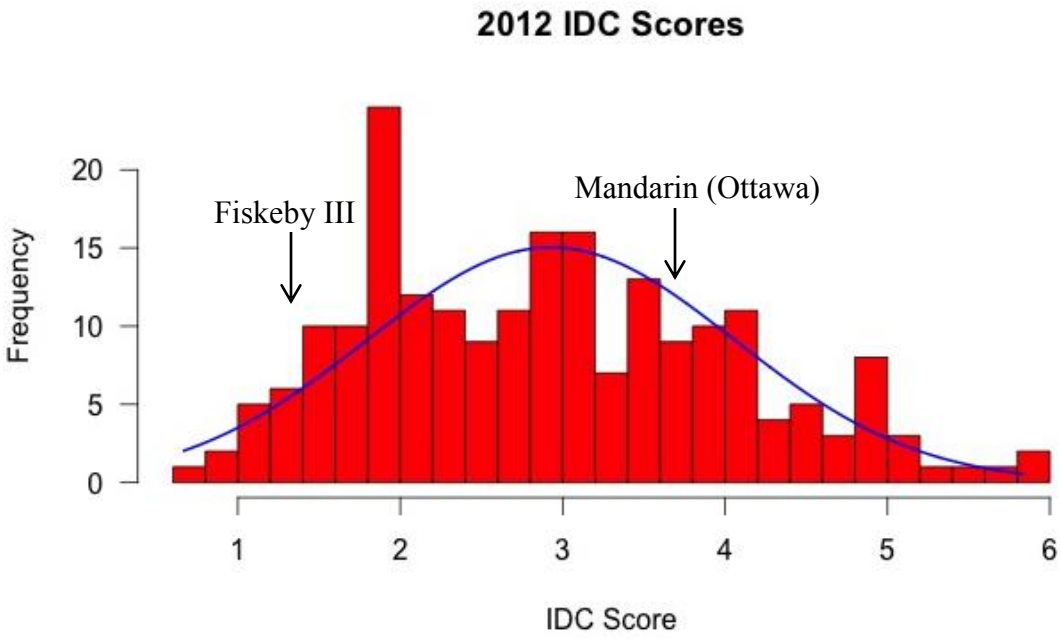

Figure 4: Distribution of iron deficiency chlorosis scores in 2013 with normality curve plotted. Scores represent an average of two repetitions taken on a 1-9 scale.

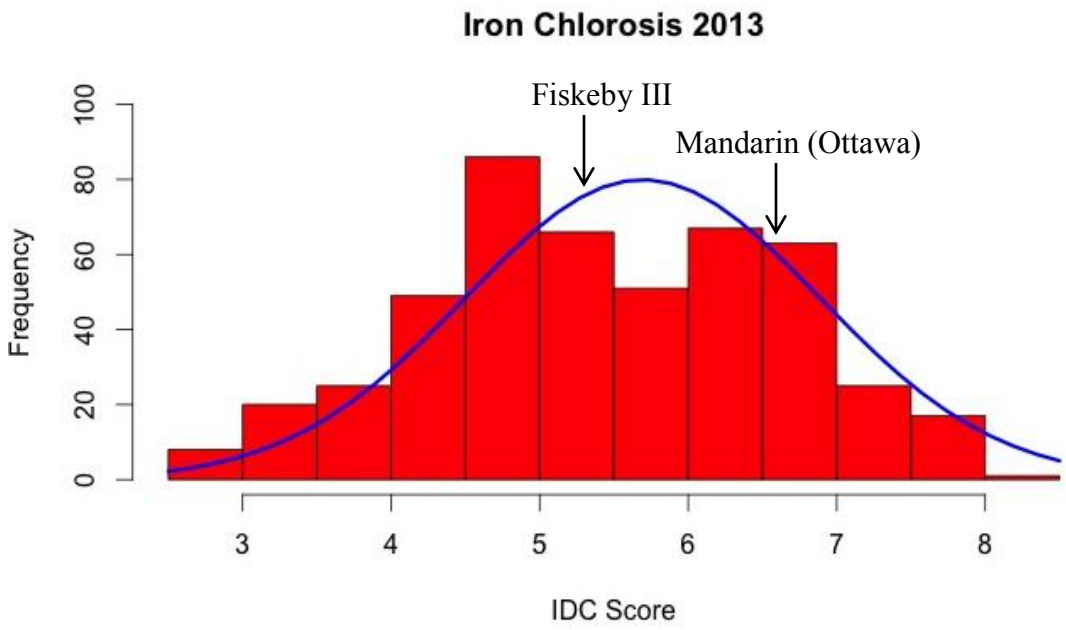

Figure 5: Distribution of iron deficiency chlorosis average scores across three years with normality curve plotted. Scores represent an average of three repetitions in 2011 and 2012 and two repetitions in 2013 taken on a 1-9 scale.

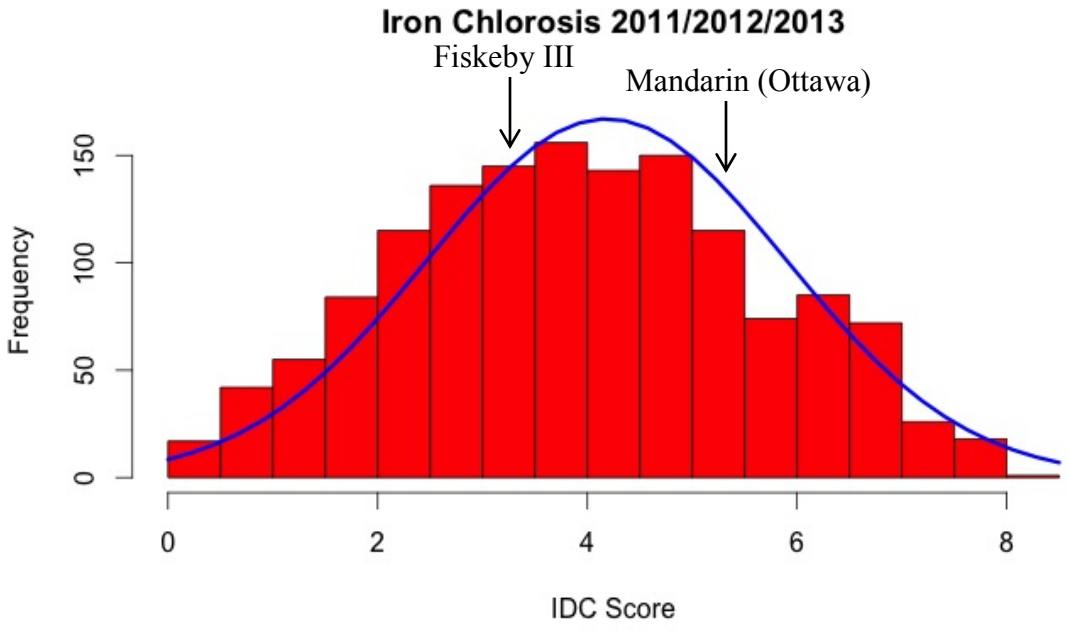

Figure 6: Marker effect plot indicating the effect of alleles from Fiskeby III and Mandarin (Ottawa) at the 044481-08709 SNP locus on the recombinant inbred line population. Values on the "Y" axis indicate the average IDC score of recombinant inbred lines carrying alleles from the denoted parent.

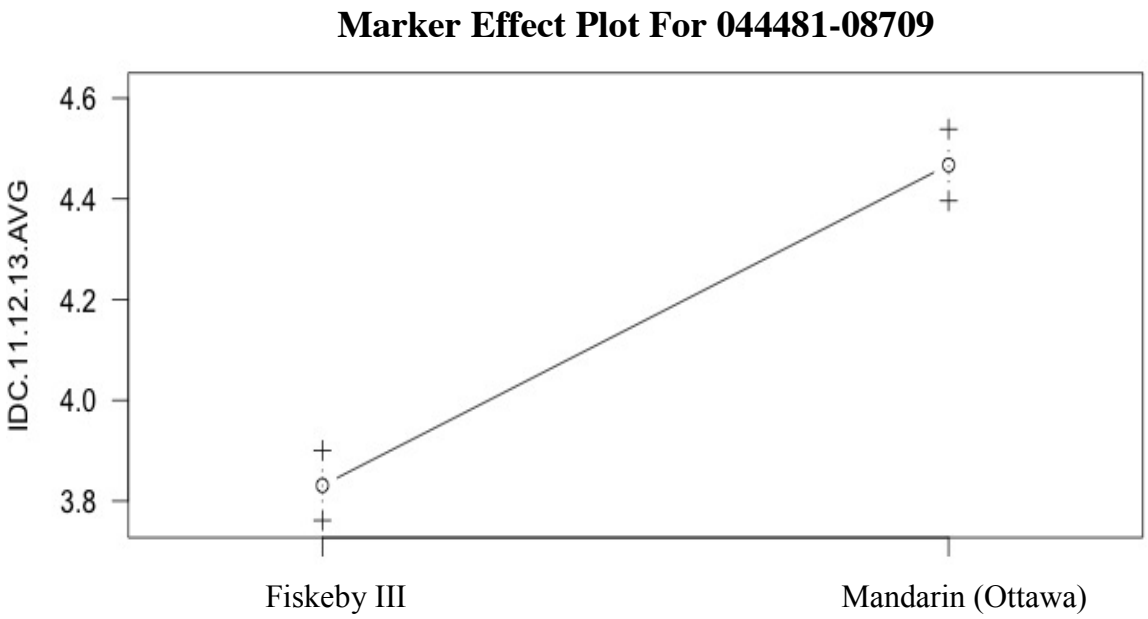

Figure 7: Marker effect plot indicating the effect of alleles from Fiskeby III and Mandarin (Ottawa) at the 014557-01578 SNP locus on the recombinant inbred line population. Values on the "Y" axis indicate the average IDC score of recombinant inbred lines carrying alleles from the denoted parent.

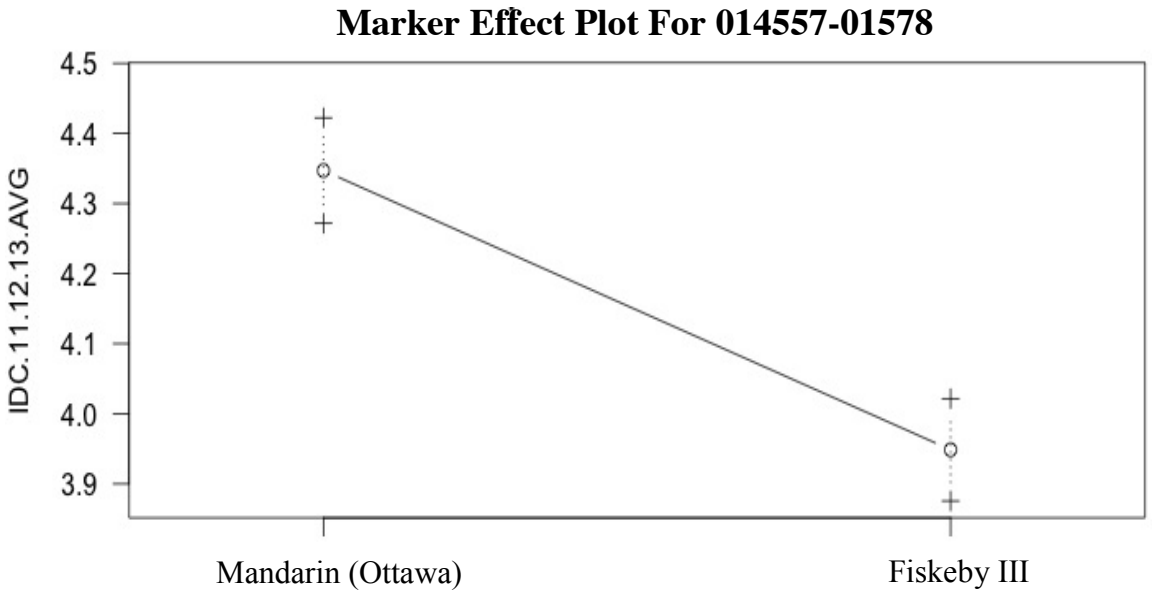

Figure 8: Genetic map of the Fiskeby III X Mandarin (Ottawa) recombinant inbred line population. The distribution of the 366 genotyped markers are shown. Q1 and Q2 indicate the location of the detected QTL for iron deficiency chlorosis.

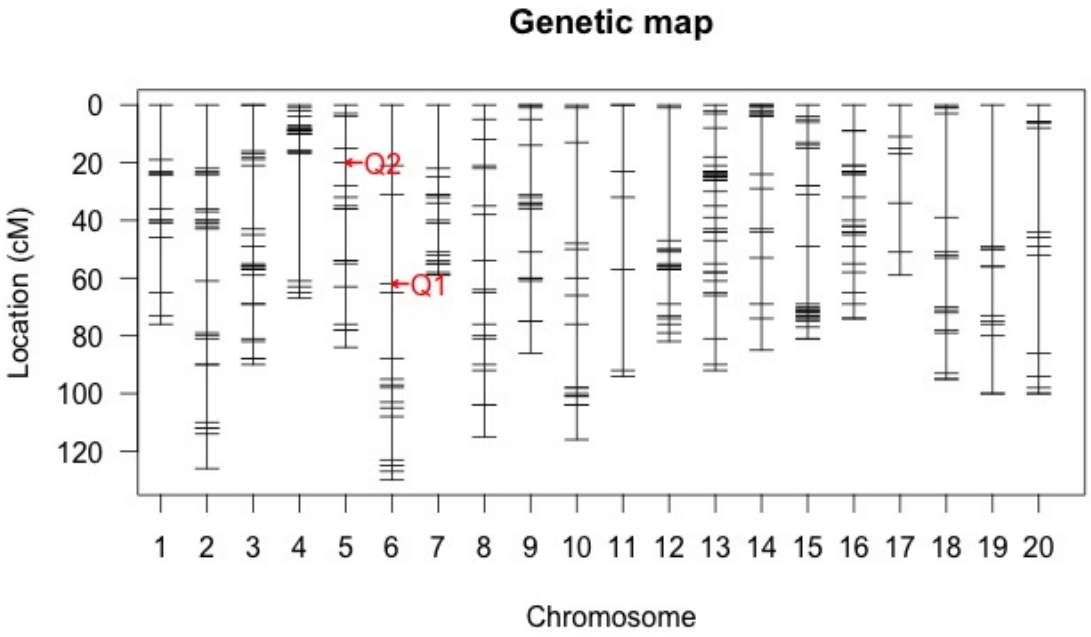

Chapter 3: Canopy Wilt QTL Mapping and Characterization of the Fiskeby III X Mandarin (Ottawa) Recombinant Inbred Line Population

Introduction

A lack of water during the soybean growing season is the most common abiotic stress that results in reduced yields (Boyer, 1982). Rainfall can be unpredictable and vary greatly between growing seasons. It has been shown that water deficits can decrease soybean yields up to 36% on an annual basis within major soybean production regions in North America (Specht et al., 1999). The Intergovernmental Panel on Climate Change (IPCC) predicts an increase in extreme weather events in the near future, including drought (Stocker et al., 2013). Some soybean production areas that currently rely on rain fed conditions may become increasingly arid, thus increasing the demand for irrigation. However, irrigation may not be economically feasible due to the high cost and limited availability of fresh water in many areas. Therefore, other avenues must be taken in order to increase the soybean's water use efficiency and tolerance to unpredictable water stressed growing conditions.

An important aspect for the continued increase of soybean yields under more variable environmental conditions will be the identification and utilization of drought tolerant germplasm in public and private breeding programs. A trait that has been identified and successfully utilized to increase yield under drought conditions is delayed canopy wilt. PI 416937 has been identified to be slow wilting and has been integrated into the background of several southern breeding lines in an attempt to increase drought tolerance (Paris, 2003). However, there is no comparable soybean line that has been utilized to increase drought tolerance via slow canopy wilt in northern germplasm. Fiskeby III, a 000 maturity group soybean, has been found to display a delayed canopy wilt phenotype under water stressed conditions, in addition to tolerance to several other

abiotic stresses (Burkey and Carter, 2009). Due to the rare occurrence of tolerance to a number of abiotic stresses, Fiskeby III presents an opportunity to study potential co-localization of abiotic stress QTL and develop a deeper understanding of soybean's response to these stresses. The identification of canopy wilt QTL in Fiskeby III will provide breeders with another tool that may lead to improved drought tolerance in early maturing soybeans. The objectives of this chapter are to (i) characterize the Fiskeby III X Mandarin (Ottawa) RIL population for the delayed canopy wilt phenotype; (ii) identify quantitative trait loci (QTL) via composite interval mapping for canopy wilt in the RIL population; and (iii) identify co-localization of canopy wilt QTL with other abiotic stress QTL, specifically, iron deficiency chlorosis.

Materials and Methods

Mapping Population and Genotyping

The same $F_{5:6}$ population of 239 recombinant inbred lines utilized in chapter two, which was derived from the hybridization of the slow wilting soybean Fiskeby III (PI 438471, maturity group 000) and the early wilting Mandarin (Ottawa) (PI 548379, maturity group 0), was used in this study. For a description of how the population was genotyped, see chapter two, "Genotypic Evaluation."

Experimental Design

The 239 recombinant inbred lines (RILs) were planted in an ongoing drought nursery in Becker, Minnesota in 2011, 2012, 2013, and 2014. This location was chosen due to the extremely sandy nature and low water holding capacity of the soil (Hubbard loamy sand, sandy mixed Udorthentic Haplorborall). A randomized complete block

design was used to plant the RILs. Plots were planted on 3 May in 2011, 11 May in 2012, 28 May in 2013, and 6 May in 2014. All plots were planted using 75 centimeter row spacing, were 90 centimeters in length, and 25 seeds were planted per plot. Plots were replicated three times throughout the nursery in 2011 and 2012, but only once in 2013 and 2014 due to lack of seed. Seven check lines were utilized each year in the field including Fiskeby III (RIL parent, resistant), Mandarin (Ottawa) (RIL parent, susceptible), 'MN0095' (resistant check), 'Sheyenne' (resistant check), 'Dawson' (susceptible check), 'Corsoy 79' (susceptible check), and 'Parker' (susceptible check).

Phenotypic Evaluation

Adequate soil moisture was maintained from planting until flowering via overhead irrigation. Once flowering was initiated, irrigation was discontinued. Plots were scored for wilting as soon as the most susceptible check (Mandarin Ottawa) showed signs of water stress. Wilting scores were measured and recorded as an average of each plot utilizing a 0 to 5 rating scale, where a score of 0 = no wilting, 1 = top few leaves wilted, 2 = 25% of the plant wilted, 3 = 50% of the plant wilted, 4 = 75% of the plant wilted and some leaf drop, and 5 = 100% of the plant wilted and considerable leaf drop. Plots were scored on 12 and 16 July in 2012, 17 and 23 July and 3 August in 2013, and 24 and 31 July and 8 August in 2014. Plots were only scored twice in 2012 due to a natural rainfall occurrence after the second scoring date. Natural rainfall in 2011 prevented the collection of reliable data, so data from 2011 was not included in the analysis.

Statistical Analysis

R Studio, version 0.97.449 (R Development Core Team, 2012) was utilized to carry out statistical analyses. An overall average wilting score was calculated for each RIL by taking the average of the three repetitions over the two scoring dates in 2012 and three scoring dates in 2013 and 2014. Results from an analysis of variance (ANOVA) were used to calculate the narrow sense heritability on an entry mean basis. The following equation was used to calculate heritability:

$$h^2 = \sigma_G^2 / [(\sigma_e^2 / ry) + (\sigma_{GY}^2 / y) + (\sigma_G^2)]$$

h^2 is the narrow sense heritability on an entry mean basis

σ_G^2 is the genetic variance

σ_e^2 is the error variance

σ_{GY}^2 is the variance of the genotype by year interaction

r is the number of repetitions

y is the number of years

A restricted maximum likelihood (REML) approach in R was used to estimate variance components. The following mixed model was used to calculate LS-means for the RILs across and within years. Replications, years, and genotypes were treated as random variables.

$$Y_{jkm} = \mu + R(E)_{k(j)} + E_j + G_m + GE_{mj} + e_{jkm}$$

Y_{jkm} is the wilting score in the *j*th year, *k*th replication, and *m*th genotype

μ is the overall mean wilting score

$R(E)_{k(j)}$ is the random effect of the *k*th replication nested in the *j*th year

E_j is the random effect of the *j*th year

G_m is the random effect of the *m*th genotype

GE_{mj} is the interaction of the *m*th genotype and *j*th year

e_{jkm} is the random error associated with the *j*th year, *k*th replication, and *m*th genotype

Average wilting scores were checked for normality using Q-Q plots and tests of skewness and kurtosis in R. Q-Q plots indicated normality for all data and skewness and kurtosis was minimal, therefore, no further data transformations were necessary.

Quantitative Trait Loci (QTL) Mapping

Composite interval mapping (CIM) in the R/qtl (Broman et al., 2003) statistical package was utilized to map quantitative trait loci (QTL) in the bi-parental Fiskeby III X Mandarin (Ottawa) population. The "cim" function in R/qtl uses a scheme from QTL Cartographer in which forward selection is first done at the markers, and then interval mapping is carried out with the selected markers as covariates. Selected marker covariates are dropped if they are located within a fixed window size of the position being tested (Broman et al., 2003). Composite interval mapping was performed using five marker covariates, a window size of 10 cM, and a walking speed of 2 cM. 1000 permutation tests were conducted using a genome-wide significance level of 0.05 in order to determine the likelihood of odds (LOD) threshold for declaring QTL significance (Doerge and Churchill, 1996). Haley-Knott regression was utilized to determine the

amount of phenotypic variation significant QTL accounted for as well as marker effect size on the 0-5 phenotypic rating scale. Mapping was carried out using an overall phenotypic mean from 2012, 2013, and 2014.

Results and Discussion

Phenotypic Characterization

Significant differences in canopy wilting scores were seen between the RILs over the three years (Table 15). The mean wilting score was 2.38, 1.68, and 2.41 in 2012, 2013, and 2014, respectively. The overall average wilting score was 2.15 for all the RILs. Canopy wilting scores followed a normal distribution over the three years tested, indicating that this trait is quantitatively inherited (Figure 9). Differences in means between the wilting tolerant parent, Fiskeby III, and the wilting susceptible parent, Mandarin (Ottawa), were also significant for the three years (Table 16). Fiskeby III's wilting score was lower than Mandarin (Ottawa's) for all repetitions in all three years, which exemplifies the consistency of their response to water deficit and confirms previous observations. The average wilting scores for Fiskeby III and Mandarin (Ottawa) over the three years were 1.31 and 3.41, respectively. Higher average wilting scores for the RILs in 2012 and 2014 compared to 2013 can most likely be explained by the weather. In the two weeks after irrigation was ceased in 2012 and canopy wilt scores were recorded, average high daily temperatures were 6.6 degrees Celsius higher than during the scoring period in 2013. In 2014, average daily highs were 3.8 degrees Celsius higher than during the scoring period in 2013. This significant difference in daily highs presumably resulted in a more rapid loss of soil moisture, increased drought stress, and more severe canopy wilt in 2012 and 2014.

The heritability on an entry mean basis was 0.66 for early canopy wilt over the three years evaluated. This was consistent with previously reported heritabilities in several canopy wilting studies in soybean (Charlson et al., 2009; Abdel-Haleem et al., 2012) Results from the ANOVA analyzing 2012, 2013, and 2014 together indicated that there was a highly significant ($p<0.001$) effect on early canopy wilting due to year, genotype, and repetition (Table 17). Variance components estimated via REML are represented as a percentage of the total variation (Table 18). The percentage of variation attributable to genotypes, years, and genotypes nested within years was the highest out of all factors besides error, with each factor accounting for approximately 13.5 percent of the phenotypic variation. Repetitions nested within years accounted for four percent of the variation, while the variance due to repetitions was negligible. Error variance accounted for 55.7 percent of the total variation. Spatial variation of the soil within the plots could have been a contributing factor to the large error variance. A reduction in error variance could have been realized if data was obtained from 2011 and if more than a single repetition could have been planted in 2013 and 2014. A rainout shelter would have been ideal and would have eliminated the loss of a year's worth of data, but it was not feasible for this study due to the size of the population and lack of funds.

Composite Interval Mapping of Early Canopy Wilt

Two quantitative trait loci (QTL) significantly associated with early canopy wilt were detected using the overall average wilting scores from 2012, 2013, and 2014 (Figure 12). Marker 044133-08626 located on chromosome six provided the strongest association with canopy wilt. This QTL had a peak LOD position at 93 cM with a LOD

score of 4.44. The 1.5-LOD support interval spanned from 70-100 cM while the Bayesian credible interval covered only the position of the peak LOD score at 93 cM (Table 19). This QTL explained 7.2 percent of the phenotypic variation for canopy wilt and caused a 0.14 decrease in the wilting score per allele copy at this marker locus. Therefore, plants with this marker allele had a wilting score that was 0.28 lower on average than plants without this marker allele due to the fact that the RILs were essentially homozygous at all analyzed marker loci (Figure 10).

Marker 029055-06058 on chromosome 12 was also found to be significantly associated with early canopy wilt. This QTL had a peak LOD position at 60 cM with a LOD score of 3.94. The 1.5-LOD support interval spanned from 55-74 cM while the Bayesian credible interval spanned a more narrow 60-62 cM interval (Table 19). This QTL explained 6.0 percent of the phenotypic variation for canopy wilt and caused a 0.13 decrease in the wilting score per allele copy at this marker locus. Therefore, plants with this marker allele had a wilting score that was 0.26 lower on average than plants without this marker allele due to the fact that the RILs were essentially homozygous at all analyzed marker loci (Figure 11).

Co-Localization of Canopy Wilt and Iron Chlorosis QTL

Marker 044133-08626 on chromosome six co-localized within the confidence interval of one of the QTL for iron chlorosis discovered in chapter two. Co-localization between the iron efficiency QTL and canopy wilt QTL seen in the current study may indicate a commonality between the mechanisms used to tolerate these abiotic stresses in Fiskeby III. Therefore, selecting for increased canopy wilting tolerance may also increase the soybean's tolerance to iron deficiency chlorosis. This could provide

breeders with a unique and efficient way to increase resistance to both abiotic stresses simultaneously.

Co-Localization of Chromosome 12 QTL with Previously Identified QTL

The identified QTL on chromosome 12 co-localized to the same confidence interval as a recently identified canopy wilt QTL in a soybean population derived from the cross of Benning and PI 416937 (Abdel-Haleem et al., 2012). The QTL the authors identified on chromosome 12 was the only QTL out of the seven they discovered that was significant in all five tested environments, and it explained 27% of the phenotypic variation for canopy wilt. One of the parents (PI 416937) used to create the RIL population for the study was discovered to be slow wilting during a field screening of hundreds of PIs in the 1980s (Sloane et al., 1990). Since this discovery, it has been studied extensively in order to elucidate the mechanisms it utilizes that enable it to delay canopy wilting. In addition to the delayed wilting response under drought stress, PI 416937 has been shown to maintain higher relative water content and turgor compared to elite cultivars. This characteristic resulted in only a minimal decrease in yield under normal growing conditions (Sloane et al., 1990). PI 416937 was also shown to have an extensive fibrous root structure and higher levels of nitrogenase activity (Hudak and Patterson, 1995). Under a significant vapor pressure deficit (VPD), PI 416937 maintained a constant transpiration rate while two fast-wilting cultivars increased transpiration rates as the VPD increased (Fletcher et al., 2007). This, along with a lower stomatal conductance and hydraulic conductance allow PI 416937 to conserve water under drought stress (Tanaka et al., 2010). King et al. (2009) and Ries et al. (2012) found that PI 416937 had greater soil moisture than elite cultivars during water stress and

concluded that under normal soil moisture conditions, PI 416937 had a decreased transpiration rate that allowed it to conserve water that it could utilize during drought conditions. PI 416937 originated from Japan, as did Namikawa (Sachilin), one of the parents of Fiskeby III in which the slow-wilting trait originated from in the present study. The fact that PI 416937 and Namikawa (Sachilin) share common geographic origins and that the QTL identified in this study co-localized with the PI 416937 QTL on chromosome 12, the potential for common drought tolerance mechanisms in Fiskeby III and PI 416937 exist. This hypothesis could be tested by further characterizing Fiskeby III and the RIL population for potential drought tolerance mechanisms and screening them for the known mechanisms that PI 416937 utilizes. A deeper understanding of the mechanisms Fiskeby III employs to combat drought stress could lead to an improvement in the efficiency of selecting for and transferring these traits into elite germplasm.

Two additional QTL associated with drought tolerance co-localized with the QTL on chromosome 12 discovered in the present study. Drought tolerance QTL 6-4, as identified on Soybase (www.soybase.org), was associated with the soybean's ability to limit leaf hydraulic conductance under water deficits (Carpentieri-Pipolo et al., 2011). This characteristic enables the plant to reach a maximum transpiration rate and conserve water under drought stress. The third drought related QTL that co-localized with the identified QTL in the present study was drought susceptibility index QTL 1-3 (Du et al., 2009). A drought susceptibility index (DSI) was calculated by dividing the relative yield loss for each genotype by the mean yield loss of all tested genotypes in the experiment. Plants containing QTL 1-3 had higher yields on average than plants without this QTL.

Furthermore, a large number of QTL associated with seed composition, abiotic stress, and plant development and morphology co-localized with the QTL on chromosome 12 that was found in this study. These QTL included five for seed weight (sd_wt 35-4, 13-8, 36-4, 41-1, 34-4), three for seed protein (Prot 33-1, 5-2, 21-10), two for seed oil (oil 37-5, 6-5), three for seed yield (sd_yld 11-4, 15-8, 22-4), three for iron efficiency (Fe effic 4-3, 8-3, 11-3), two for pubescence density (pub 2-14, 2-8), two for plant height (Pl_ht 13-4, 36-1), four for isoflavone components (Genistein 4-2, Glycitein 4-4, Daidzein 2-2, Isoflavone 1-3), and one for lodging (Lodg 9-2).

It was not surprising that many of these QTL co-localized. Soybeans produce more isoflavones when they are grown under irrigated soil conditions compared to dry soil conditions (Bennett et al., 2004). In addition, under long periods of drought stress, changes were seen in the expression of isoflavone related genes and isoflavone seed content (Gutierrez-Gonzalez et al., 2010). This association between drought tolerance and isoflavone content helps to explain the co-localization of the canopy wilt and genistein, glycitein, and daidzein QTL seen in the present study.

Seed yield QTL identified by Kabelka et al. (2004) that co-localized with the canopy wilt QTL could provide a means of improving yield by selecting for delayed canopy wilt. Identifying five QTL associated with seed weight that co-localized with canopy wilt is logical since water deficits during soybean flowering lead to decreased pod set and a decrease in the number of seeds per pod. This, in turn, affects the seed weight and the overall yield (Liu et al., 2003). Additionally, the co-localization of seed oil and protein QTL with the canopy wilt QTL could be explained by the fact that as drought becomes more severe, seed oil increases and seed protein decreases (Specht et al., 2001).

Pubescent density QTL could be co-localizing with canopy wilt QTL due to the possibility of pubescence playing a role in plant temperature regulation and radiation balance. Results from Nielsen et al. (1984) suggest that soybeans with dense pubescence may be better adapted to high radiation, high temperatures, and limited moisture conditions. Indeed, a major gene controlling pubescent density mapped to this QTL region and RILs that were homozygous for the semi-sparse pubescence (*Ps-s)* allele yielded 168.2 kg ha^{-1} less than RILs homozygous for the normal pubescence density allele (Specht et al., 2001).

Conclusions

Significant differences in canopy wilting scores were seen between the RILs over the three years. Average daily maximum temperatures in 2012 and 2014 that significantly exceeded those in 2013 during the scoring time frame could explain the significant differences. Fiskeby III consistently scored lower on average than Mandarin (Ottawa) over the three years for canopy wilting. A normal distribution of canopy wilting scores for the three years tested indicated that this trait is quantitatively inherited. The heritability on an entry mean basis was 0.66, which was consistent with previously reported heritabilities in several canopy wilting studies in soybean. An ANOVA indicated a significant effect due to year, genotype, and repetition. Estimation of variance components via REML exemplified that error accounted for the most variation, followed by years, genotypes, and genotypes nested within years. A reduction in error variance could have been achieved if data from 2011 was available and if more than a single repetition was available in 2013 and 2014.

Two quantitative trait loci (QTL) significantly associated with early canopy wilt were detected on chromosomes six and 12 that together explained 13.2 percent of the phenotypic variation. The QTL identified on chromosome six co-localized with one of the QTL for iron chlorosis identified in chapter two. This may indicate that Fiskeby III utilizes a common mechanism to tolerate iron chlorosis and drought stress. The chromosome 12 QTL co-localized with two previously identified QTL associated with drought tolerance as well as a number of additional QTL associated with iron deficiency chlorosis, seed composition and yield, and plant development and morphology.

Co-localization of the identified canopy wilt QTL on chromosome 12 with several other drought related QTL, that together explain a large portion of the phenotypic variance for drought tolerance, exemplify the importance of this chromosomal region for the soybeans' response to drought. It also further confirms that this identified QTL is almost certainly not the result of a false positive association. Therefore, potential exists for the utilization of this QTL for marker-assisted selection and improvement of elite breeding lines' tolerance to drought. In addition, co-localization of this QTL with several other potentially beneficial QTL may allow for the improvement of multiple traits simultaneously. However, prior to attempting to utilize this QTL for marker-assisted selection, fine mapping of the region should be conducted to narrow the confidence interval.

Table 15: Summary of canopy wilt ratings for the recombinant inbred line population across three years. Scores represent an average of three repetitions from two scoring dates in 2012 and one repetition from three scoring dates in 2013 and 2014 taken on a 0-5 wilting severity scale.

Trait	Year	Mean	SD*	Median	Minimum	Maximum	Skewness	Kurtosis
Wilt	2012	2.38	1.15	2.5	0	5	0.15	-0.68
Wilt	2013	1.68	0.53	1.67	1	3.33	0.5	-0.60
Wilt	2014	2.41	0.88	2.33	1	4.33	0.25	-0.71
Wilt	2012/2013/2014	2.15	0.97	2	0	5	0.37	-0.47

* indicates standard deviation

Table 16: Summary of canopy wilt ratings for the drought tolerant Fiskeby III, the drought susceptible Mandarin (Ottawa), and the recombinant inbred line population from 2012-2014. Scores represent an average of three repetitions in 2012 and one repetition in 2013 and 2014 for the RILs. 15 repetitions were used for Fiskeby III and Mandarin (Ottawa) in 2012 and five were used in 2013 and 2014. Scores were taken on a 0-5 wilting severity scale.

Trait	Year	Line	Mean	Minimum	Maximum
Wilt	2012	FIII*	0.94	0	3
Wilt	2012	MO**	3.9	2	5
Wilt	2012	RILs***	2.38	0	5
Wilt	2013	FIII	2.0	1	3
Wilt	2013	MO	2.34	2	4
Wilt	2013	RILs	1.68	1	3.33
Wilt	2014	FIII	1	1	1
Wilt	2014	MO	4	4	4
Wilt	2014	RILs	2.41	1	4.33
Wilt	2012/2013/2014	FIII	1.31	0	3
Wilt	2012/2013/2014	MO	3.41	2	5
Wilt	2012/2013/2014	RILs	2.15	0	5

* indicates Fiskeby III
** indicates Mandarin (Ottawa)
*** indicates recombinant inbred lines

Table 17: Analysis of variance for canopy wilt from 2012-2014.

Source	Df	Sum Sq	Mean Sq	F value	Pr(>F)
Genotype	241	435.84	1.808	2.9425	<2.2e-16***
Year	2	98.46	49.229	80.099	<2.2e-16***
Rep	2	19.88	9.939	16.1709	1.24e-07***
Residuals	968	594.93	0.615		

*** indicates significance at the 0.001 probability level.

Table 18: Variance components estimated via REML for canopy wilt from 2012-2014.

Variance Component	Standard Deviation	Variance	Percent of Total Variance (%)
Genotype	0.3649	0.133	13
Year	0.3673	0.135	14
Rep	0	0	0
Genotype:Year	0.3646	0.133	13
Rep:Year	0.2013	0.04	4
Error	0.7459	0.556	56

Table 19: Summary of results for composite interval mapping of canopy wilt in the Fiskeby III X Mandarin (Ottawa) RIL population. R^2 indicates the percent variation explained by the QTL. The sign of the additive effect refers to the Fiskeby III parent, where a positive additive effect indicates the Fiskeby III allele increases the wilting score, and a negative additive effect indicates the Fiskeby III allele decreases the wilting score. The additive effect represents the effect of a single "A" or "B" allele.

Trait	Marker	Chr	LOD Peak Position (cM)	LOD Score	1.5-LOD Support Interval (cM)	Bayesian Credible Interval (cM)	R^2 (%)	Additive Effect
Canopy Wilt	029055-06058	12	60	3.94	55-74	60-62	6.0	-0.13
Canopy Wilt	044133-08626	6	93	4.44	70-100	93	7.2	-0.14

Figure 9: Distribution of average canopy wilt scores from 2012-2014 with normality curve plotted. Scores represent an average of three repetitions in 2012 and one repetition in 2013 and 2014 taken on a 0-5 scale.

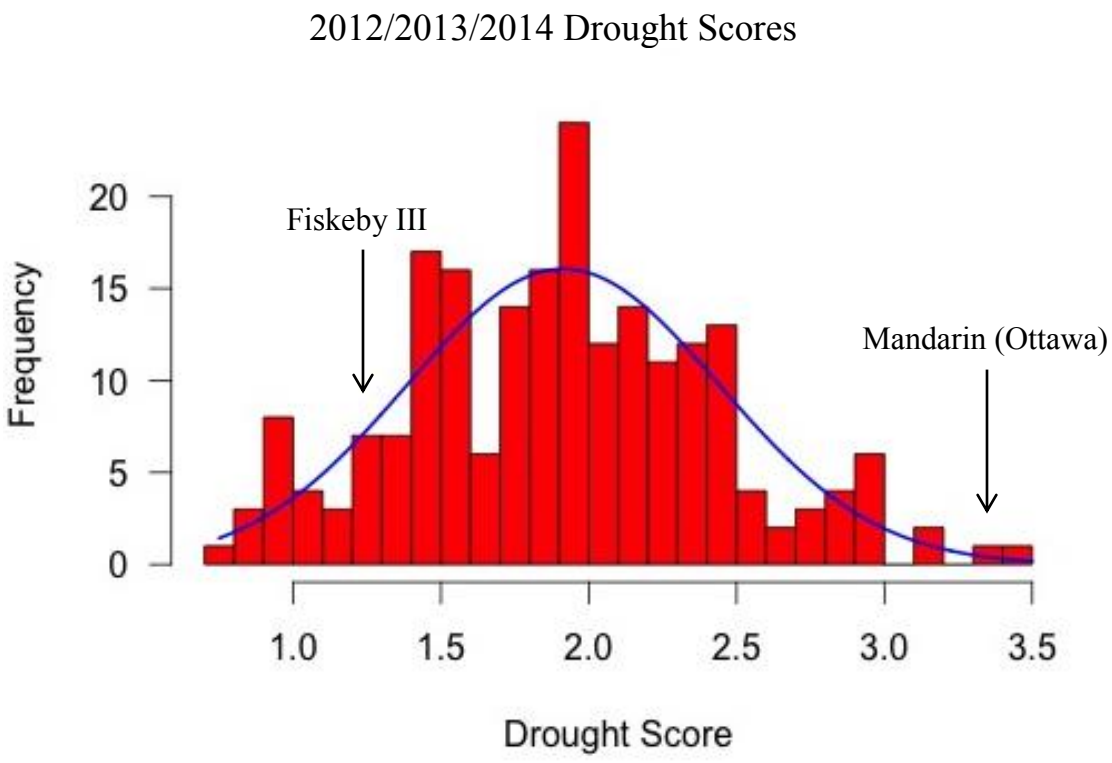

Figure 10: Marker effect plot indicating the effect of alleles from Fiskeby III and Mandarin (Ottawa) at the 044133-08626 SNP locus on the recombinant inbred line population. Values on the "Y" axis indicate the average wilt score of recombinant inbred lines carrying alleles from the denoted parent.

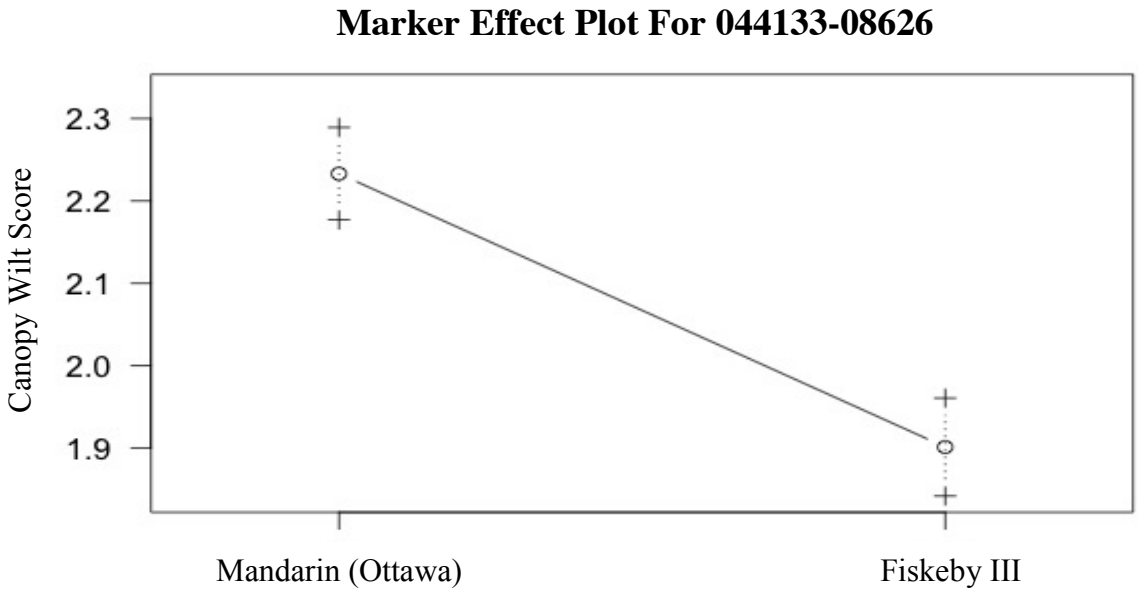

Figure 11: Marker effect plot indicating the effect of alleles from Fiskeby III and Mandarin (Ottawa) at the 029055-06058 SNP locus on the recombinant inbred line population. Values on the "Y" axis indicate the average wilt score of recombinant inbred lines carrying alleles from the denoted parent.

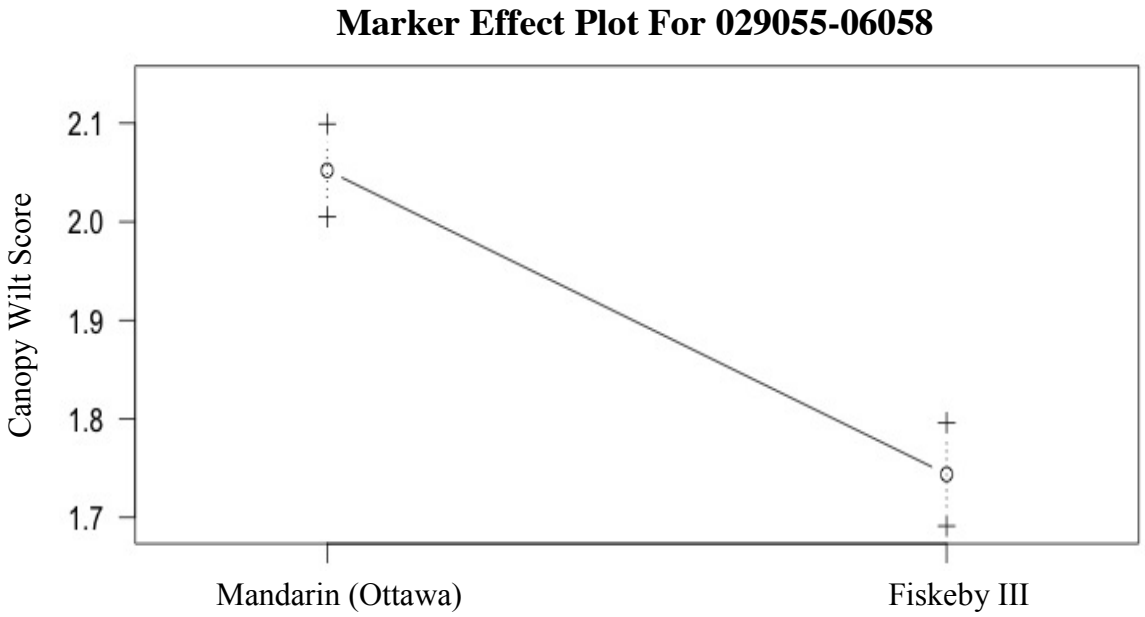

Figure 12: Genetic map of the Fiskeby III X Mandarin (Ottawa) recombinant inbred line population. The distribution of the 366 genotyped markers are shown. Q1 indicates the location of the detected QTL for canopy wilt on chromosome 6 and Q2 indicates the QTL on chromosome 12.

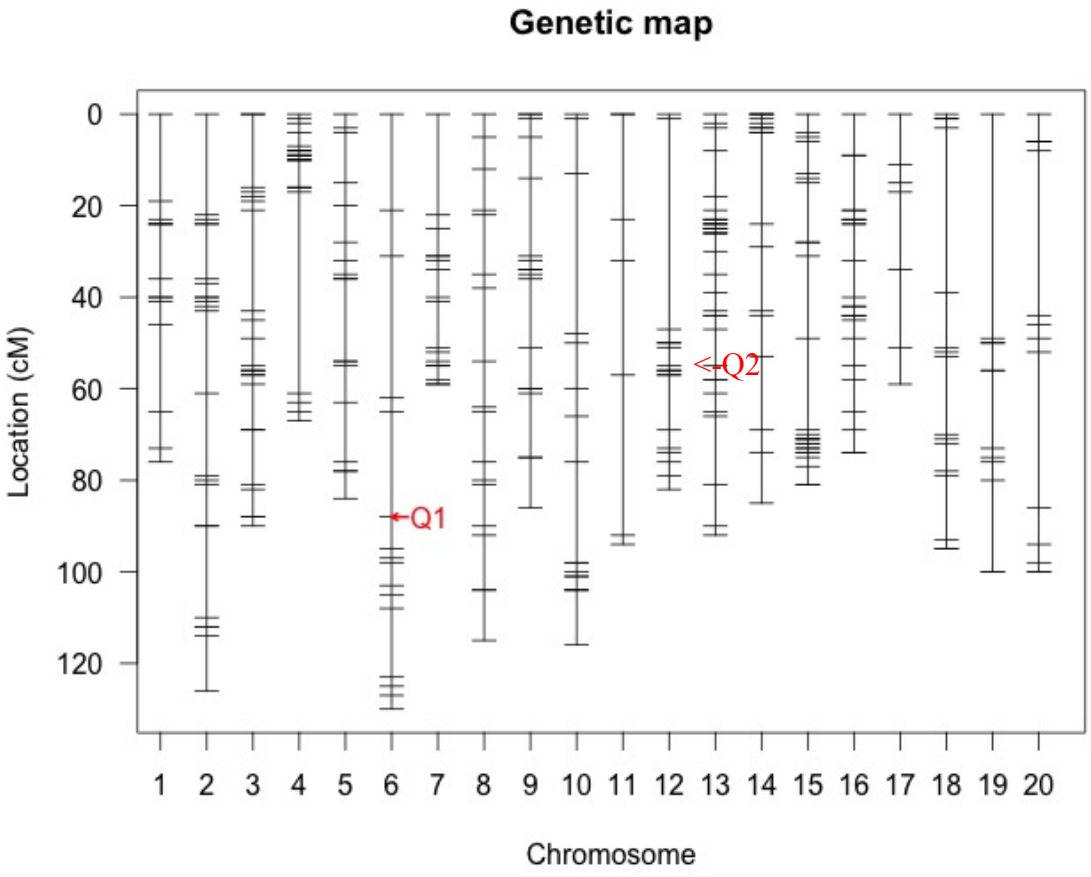

Chapter 4: Genome Wide Association Study for QTL Validation of Iron Deficiency Chlorosis

Introduction

The majority of QTL mapping experiments in plants have largely been focused on linkage mapping in single bi-parental populations. Bi-parental mapping populations are beneficial because they allow for the control of population structure, which reduces the probability of detecting false positive marker-trait associations. However, the effects of QTL identified in small bi-parental mapping populations are often overestimated (Beavis, 1998). In addition, QTL detected in bi-parental populations tend to be population specific, in that a QTL detected in one population may not be detected in an unrelated population. This could be the result of genetic heterogeneity; when many genes control a trait, different subsets of genes can segregate in different populations (Holland, 2007). Linkage analysis also has comparably poor resolution due to the limited amount of recombination events that can occur during the construction of bi-parental mapping populations. Average QTL intervals are between 10 and 20 cM (Holland, 2007). This level of resolution makes it extremely difficult to identify candidate genes without further fine mapping of the QTL region.

More recently, association mapping has gained popularity in mapping experiments. Association mapping, unlike bi-parental mapping, is advantageous because it allows for the exploitation of historical recombination events so that greater mapping resolution can be achieved (Risch and Merikangas, 1996; Nordborg and Tavaré, 2002). In addition, populations evaluated by association mapping tend to consist of diverse sets of lines, which results in the sampling of a greater amount of allelic diversity than in traditional bi-parental mapping. An important consideration is whether or not association mapping and traditional QTL mapping can detect the same loci underlying a trait (Wang

et al., 2008). In association mapping, an allele must be present at a high enough frequency in the population being evaluated to be detected.

The current study was undertaken because two independent populations were identified on the Germplasm Resource Information Network (USDA, ARS, National Genetic Resources Program, 2014) website that had the potential of containing several lines with Fiskeby III in their genetic backgrounds. All the lines had phenotypic data for IDC, and genotypic data was available on SoyBase (www.soybase.org). Therefore, with this data, there is potential to utilize association mapping to validate the QTL identified for IDC in the Fiskeby III X Mandarin (Ottawa) RIL population in chapter two. The objectives of this chapter are to (i) utilize association mapping to detect markers significantly associated with IDC in two independent populations, (ii) compare significant identified markers with the QTL regions identified in chapter two, and (iii) validate the major QTL identified on chromosome five in chapter two.

Materials and Methods

Phenotypic Data

All phenotypic data utilized in this study was obtained from the Germplasm Resource Information Network (USDA, ARS, National Genetic Resources Program, 2014) website. Two independent populations consisting of plant introductions and soybean breeding lines developed by public breeding programs for Canada and the Northern United States were evaluated. The first population consisted of 1341 maturity group I soybeans planted in Boyd and Morgan, Minnesota in 2001. Two repetitions were planted at both locations, and iron chlorosis severity scores were taken twice during the course of the growing season. The second population consisted of 387 maturity group 0

soybeans planted in five locations in 2004. The locations included Buffalo Lake, Sleepy Eye, Woodlake, and two separate sites in Morgan, Minnesota. Three repetitions were planted at all locations, and plots were scored twice throughout the growing season. Both populations were scored using a 1-5 chlorosis severity rating scale where 1 indicated no chlorosis and 5 indicated severe chlorosis. Final scores for both populations were reported as least square means using neighboring plots as covariates to adjust the means. Phenotypic data from the two populations was analyzed separately with an analysis of variance (ANOVA) in R (R Development Core Team, 2010) in order to determine the effects of genotypes and locations.

Genotypic Data

Genotypic data was downloaded from SoyBase (www.soybase.org). All accessions were genotyped using the SoySNP50K iSelect SNP beadchip (Song et al., 2013). Of the 1341 accessions that were phenotyped in 2001, only 693 accessions had genotypic information available. Two hundred fifty-seven accessions from the 2004 phenotypic data had genotypic data available. Therefore, only lines with available phenotypic and genotypic data were used in the analysis. SNP calls were filtered out if they had a missing data rate greater than 50% or a minor allele frequency (MAF) of 5% or less. Twenty-six thousand, eight hundred and eighty-nine SNP markers were retained for the 2001 analysis, and 25,028 SNP markers were retained for the 2004 analysis after filtering.

Association Mapping

Principal component analysis (PCA) in R (R Development Core Team, 2010) was

implemented to control for population structure in the 2001 and 2004 populations separately (Price et al., 2006). The number of principal components (eigenvectors per combination of SNP markers) that jointly explained 20% of the variation were selected to be used in the analysis. An additive relationship matrix to estimate kinship was also calculated using the "rrBLUP" package in R (R Development Core Team, 2010).

Association mapping was carried out using the Population Structure + Kinship (PCA+K) model in the "rrBLUP" package in R (R Development Core Team, 2010), which utilizes the mixed-model described by Yu et al. (2006). Results from the PCA indicated that the first three principal components accounted for >20% of the variation in both the 2001 and 2004 data, therefore, three principal components were used to control population structure in the analysis. The results from association mapping were imported into SNPEVG (Wang et al., 2012) to create Manhattan plots. Markers with likelihood of odds (LOD) scores greater than three in at least three environments were considered significant. A forward stepwise linear regression model with the chlorosis scores as dependent variables and the significant SNP markers as explanatory variables was constructed in R (R Development Core Team, 2010). The model was used to estimate the percentage of variation explained by each significant SNP marker and all significant markers simultaneously. Due to the fact that the significant SNP markers were pre-selected in the linear regression model, the r^2 estimates were likely up-biased.

Results and Discussion

Phenotypic Analysis

Tests for skewness and kurtosis indicated that the phenotypic data from both the 2001 and 2004 was normally distributed. As expected with iron chlorosis, a wide range of variation was seen between the years and genotypes. The 2001 population had a range of IDC scores from 1 to 5 with a mean of 3.12, while the 2004 population scores ranged from 1 to 5 with a mean of 3.55. Results from the ANOVA demonstrated a highly ($p<0.001$) significant effect for genotypes and locations in both the 2001 (Table 20) and 2004 (Table 21) populations.

Association Mapping

Population structure was analyzed using principal component analysis (PCA) for the 2001 and 2004 populations separately (Price et al., 2006). In 2001, 21.5% of the variance was explained by the first three principal components, where 9.5, 6.5, and 5.5% of the variance was explained by the first through third principal components, respectively (Figure 13). In 2004, 29.5% of the variance was explained by the first three principal components, where 15.5, 8, and 6% of the variance was explained by the first through third principal components, respectively (Figure 14).

Upon utilizing PCA to account for population structure in the model, association mapping led to the discovery of 12 SNP markers significantly associated with iron deficiency chlorosis (Table 22). These 12 markers were found to be significant (LOD>3) across at least three locations throughout the two tested years (Figures 15 and 16). Results from the forward stepwise linear regression pre-selecting the 12 significant

markers in the model indicated that these markers accounted for 27.2 percent and 8.9 percent of the phenotypic variation in the 2004 and 2001 populations, respectively. Significant markers were located on chromosomes 3,5,18,19, and 20. Although 12 markers were found to be significant, markers on chromosome 3,5,18, and 19 clustered together leading to a single unique region identified on each of the five chromosomes. Marker ss715638021 located on chromosome 20 was unique to the 2001 population, and the three significant markers located on chromosome 18 and two significant markers located on chromosome 19 were unique to the 2004 population. The region with significant markers located on chromosomes 3 and 5 were identified in both the 2001 and 2004 population.

Co-localization of Significant Markers with Previously Identified QTL

Significant markers in the current study co-localized with several previously identified IDC QTL as well as several known iron related genes. A major IDC QTL on chromosome three was previously identified that accounted for more than 70 percent of the phenotypic variation for IDC (Lin et al., 1997, 2000). The authors hypothesized that IDC was controlled by a single major gene in the specific bi-parental mapping population. Research with the near isogenic soybean lines Clark and iso-Clark recently confirmed that an introgression on chromosome three from the iron inefficient donor line (T203) co-localized with this major QTL (Severin et al., 2010). This introgression was mapped between 36.3 and 45.8 Mbp on chromosome three. The significant markers in the current study on chromosome three were located between 36.2 and 36.6 Mbp. These markers most likely are associated with the same gene/genes that have previously been reported to affect the iron chlorosis response in soybean in this region. Peiffer et al.

(2012) recently identified two candidate genes encoding transcription factors that are located only 250kb upstream of the significant markers identified on chromosome three in the current study. One of these genes (Glyma03g28610) was found to contain a 12 base pair deletion that was common to all of the iron inefficient lines in the study. The authors came to the conclusion that the deletion disrupted the Fe-deficiency-induced transcription factor (FIT)/bHLH heterodimer that has been shown to induce known iron acquisition genes (Peiffer et al., 2012). These results supported the previous hypothesis by O'Rourke et al. (2009) that regulatory elements within the known chromosome three iron QTL were responsible for gene expression changes of known iron genes located outside the QTL region. Lastly, Mamidi et al. (2011) recently identified another potential candidate gene in this chromosome three QTL region. The gene, *NAS3*, encodes for an enzyme that synthesizes the carrier that transports iron from old leaves into young leaves and flowers. Loss of function of this gene may lead to decreased movement of iron throughout the plant and chlorotic symptoms in young leaves.

In addition, the significant markers identified in the current study on chromosome 19 co-localized with another known iron related gene. This gene is part of the oligopeptide transporter (OPT) gene family and has been shown to play a role in whole-plant iron homeostasis and loading of iron into developing seeds (Stacey et al., 2008).

Validation of Major Chromosome Five IDC QTL

The most significant finding in chapter two was the identification of a major QTL for IDC tolerance that explained nearly 20 percent of the phenotypic variation for IDC in the Fiskeby III X Mandarin (Ottawa) RIL population. The primary goal of this chapter

was to validate this QTL using publically available phenotypic and genotypic data from several independent populations. Association mapping led to the discovery of a group of 11 significant markers spanning approximately 280kb that clustered together on chromosome five (Table 23). Three of these markers were found to be significant in three different environments and combined environment analyses. The significant markers co-localized to the same region as the major QTL identified in chapter two on chromosome five. Results from forward stepwise linear regression pre-selecting the 11 significant markers in the model indicated that these markers accounted for 14.7 percent of the phenotypic variation for IDC. These results concurred with the amount of variation the major QTL accounted for in chapter two. Pre-selecting only the three markers that were found to be significant across populations in the model indicated that these three markers accounted for 9.3 percent of the variation.

In addition to the potential candidate gene, ferredoxin thioredoxin reductase (FTR), identified in chapter two on chromosome five, another potential candidate gene was identified as a result of association mapping (Table 13). Glyma05g09210 is located 100 kb upstream from the FTR candidate gene found in the major chromosome five QTL, and is a member of the multidrug and toxin efflux protein family (MATE). The ferric reductase defective (FRD3) protein in *Arabidopsis*, which is a member of the MATE family, has been shown to play an important role in iron translocation and the overall iron response of strategy one plants (Rogers and Guerinot, 2002; Durrett et al., 2007). Mutant FDR3 plants exhibited a chlorotic phenotype and a constitutive iron uptake response. Although there was an increased uptake of iron by the mutant plants, leaf tissues had decreased iron concentrations. This led the authors to conclude that FDR3 effluxes

citrate into the root vasculature, which forms a complex with iron. The ferric-citrate complex is then transported through the xylem to growing parts of the plant (Durrett et al., 2007). Expression data for soybean published on SoyBase (www.soybase.org) illustrated that Glyma05g09210 is expressed almost exclusively in the roots, which would follow logic if it had similar activity to FDR3 (Table 14). Expression levels of this gene should be compared in Fiskeby III and Mandarin (Ottawa) to see if there are any significant differences under normal iron and low iron conditions, and the gene should also be sequenced to determine if there are any mutations in this gene in either of the parents. Expression and sequencing results would help to confirm whether or not Glyma05g09210 plays a role in the chlorotic phenotype observed in this population.

Conclusions

The principal components analysis plus kinship model (PCA+K) was utilized to decrease the probability of spurious marker-trait associations due to population structure during the association mapping. Three subpopulations were identified in both the 2001 and 2004 populations. Association mapping using three subpopulations in the model identified 12 significant markers that accounted for 27.2 percent and 8.9 percent of the phenotypic variation for IDC in the 2004 and 2001 populations, respectively. These markers co-localized with several known iron related QTL and genes. A significant cluster of 11 markers on chromosome five co-localized with the major IDC QTL identified in chapter two. Stepwise linear regression indicated that these 11 markers accounted for 14.7 percent of the phenotypic variation for IDC. A second candidate gene, Glyma05g09210, was identified on chromosome five that belongs to the MATE family of proteins. Members of this gene family have been shown to play an important

role in the translocation of iron in *Arabidopsis* (Rogers and Guerinot, 2002; Durrett et al., 2007).

The Co-localization of significant markers in this study with previously identified IDC QTL and iron related genes exemplifies the efficacy of the PCA+K model to account for population structure and confirms the accuracy of our results. Furthermore, co-localization of a cluster of significant markers with the major IDC QTL on chromosome five validates the discovery of this QTL and further demonstrates its potential for marker-assisted selection to improve IDC tolerance in elite soybean breeding material.

Table 20: Analysis of variance for IDC in the 2001 population.

Source	Df	Sum Sq	Mean Sq	F value	Pr(>F)
Genotype	692	543.81	0.786	1.5465	5.6e-09***
Location	1	95.12	95.12	187.2	<2.2e-16***
Residuals	692	351.63	0.508		

*** indicates significance at the 0.001 probability level.

Table 21: Analysis of variance for IDC in the 2004 population.

Source	Df	Sum Sq	Mean Sq	F value	Pr(>F)
Genotype	360	270.47	0.751	1.2671	0.0025**
Location	4	50.76	50.76	85.6169	<2.2e-16***
Residuals	1049	621.98	0.593		

***,** indicates significance at the 0.001 and 0.01 probability levels, respectively.

Table 22: Markers significantly associated with IDC in the 2001 and 2004 populations. SNP identification number, chromosome number, genetic position in basepairs, and maximum LOD score for each marker over all locations is given.

SNP ID	Chromosome	Position (bp)	Maximum LOD Score
ss715585425	Gm03	36265203	7.1
ss715585427	Gm03	36267507	6.5
ss715585486	Gm03	36634361	6.0
ss715592597	Gm05	8825498	3.7
ss715592598	Gm05	8826076	3.7
ss715592610	Gm05	8916450	3.6
ss715630470	Gm18	3925060	4.6
ss715630474	Gm18	3941529	5.0
ss715630498	Gm18	4083379	4.1
ss715635231	Gm19	42655124	4.7
ss715635235	Gm19	42693901	4.7
ss715638021	Gm20	38214430	4.0

Table 23: Markers significantly associated with IDC on chromosome five. SNP identification number, chromosome number, genetic position in basepairs, and maximum LOD score for each marker is given.

SNP ID	Chromosome	Position (bp)	Maximum LOD Score
ss715592597	Gm05	8825498	3.7
ss715592598	Gm05	8826076	3.7
ss715592610	Gm05	8916450	3.6
ss715592615	Gm05	8956994	3.5
ss715592620	Gm05	8994312	3.1
ss715592622	Gm05	9000470	3.1
ss715592623	Gm05	9012813	3.1
ss715592626	Gm05	9059149	3.5
ss715592627	Gm05	9066302	3.7
ss715592632	Gm05	9097414	3.4
ss715592634	Gm05	9107146	3.8

Figure 13: Plot of the results of principal components analysis in the 2001 population. The first 10 principal components are plotted on the X-axis. The fraction of variance each principal component explains is plotted on the Y-axis.

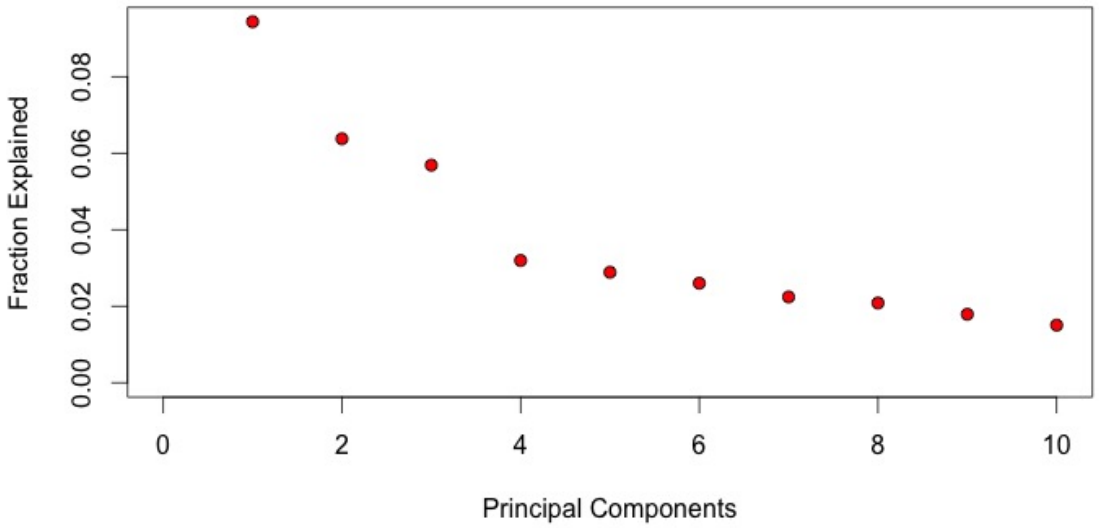

Figure 14: Plot of the results of principal components analysis in the 2004 population. The first 10 principal components are plotted on the X-axis. The fraction of variance each principal component explains is plotted on the Y-axis.

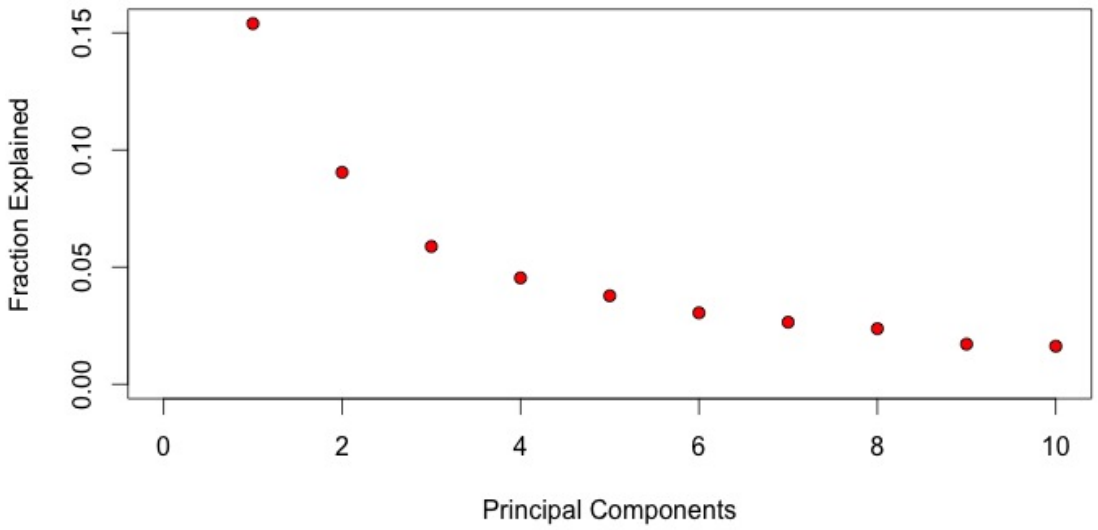

Figure 15: Manhattan Plot displaying the results of association mapping for the 2001 population. The 20 chromosomes of soybean are displayed on the X-axis, and the corresponding LOD score for each marker is displayed on the Y-axis.

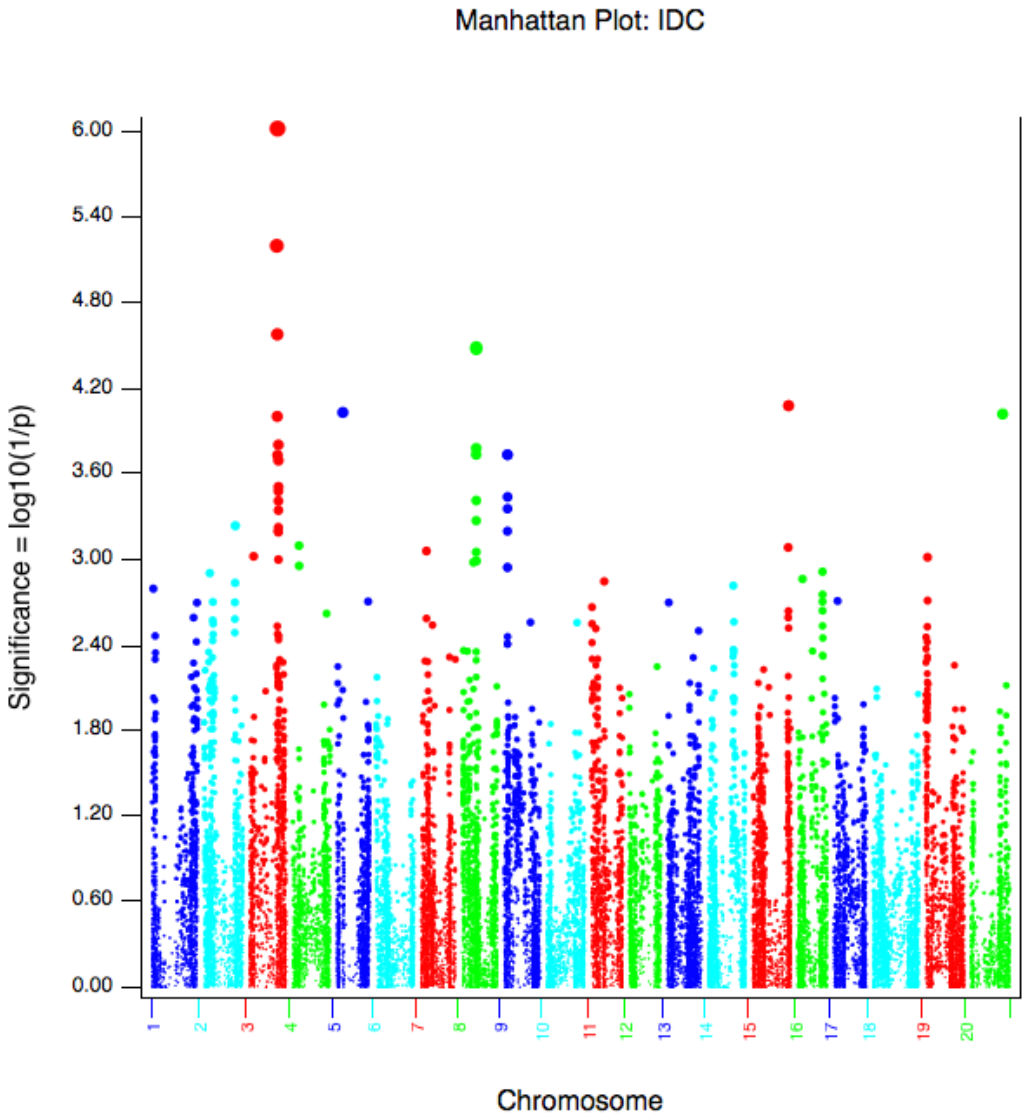

Figure 16: Manhattan Plot displaying the results of association mapping for the 2004 population. The 20 chromosomes of soybean are displayed on the X-axis, and the corresponding LOD score for each marker is displayed on the Y-axis.

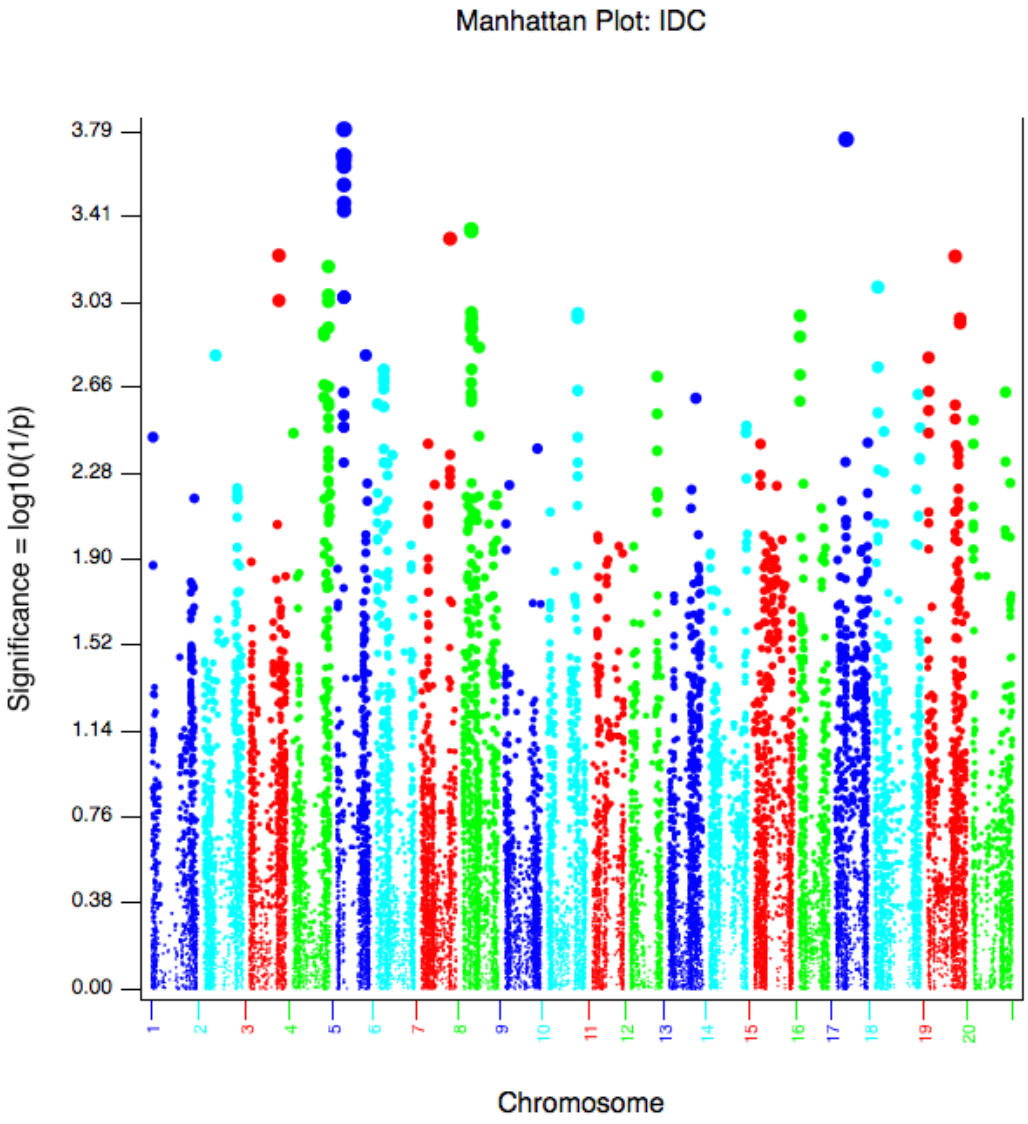

Literature Cited

Abdel-Haleem, H., T.E. Carter, L.C. Purcell, C.A. King, L.L. Ries, P. Chen, W. Schapaugh, T.R. Sinclair, and H.R. Boerma. 2012. Mapping of quantitative trait loci for canopy-wilting trait in soybean (Glycine max L. Merr). Theor. Appl. Genet. 125(5): 837–46.

Aktaş, M., and F. Egmond. 1979. Effect of nitrate nutrition on iron utilization by an Fe-efficient and an Fe-inefficient soybean cultivar. Plant Soil 51(2): 257–274.

Ambler, J.E., J.C. Brown, and H.G. Gauch. 1970. (1971) Sites of Iron Reduction in Soybean Plants (AJ). : 1970–1972.

Balmer, Y., A. Koller, G. del Val, W. Manieri, P. Schürmann, and B.B. Buchanan. 2003. Proteomics gives insight into the regulatory function of chloroplast thioredoxins. Proc. Natl. Acad. Sci. U. S. A. 100(1): 370–5.

Beavis, W.D. 1998. QTL analyses: power, precision, and accuracy. Mol. dissection complex Trait. 1998: 145–162.

Bennett, J.M., T.R. Sinclair, R.C. Muchow, and S.R. Costello. 1987. Dependence of Stomatal Conductance on leaf Water Potential, Turgor Potential, and Relative Water Content in Field-Grown Soybean and Maize1. Crop Sci. 27(5): 984.

Bennett, J.O., O. Yu, L.G. Heatherly, and H.B. Krishnan. 2004. Accumulation of genistein and daidzein, soybean isoflavones implicated in promoting human health, is significantly elevated by irrigation. J. Agric. Food Chem. 52(25): 7574–9.

Bernard, D.G., Y. Cheng, Y. Zhao, and J. Balk. 2009. An allelic mutant series of ATM3 reveals its key role in the biogenesis of cytosolic iron-sulfur proteins in Arabidopsis. Plant Physiol. 151(2): 590–602.

Bhatnagar, S., C.A. King, L. Purcell, and J.D. Ray. 2005. Identification and mapping of quantitative trait loci associated with crop responses to water-deficit stress in soybean [Glycine max (L.) Merr.]. *In* The ASACSSA-SSSA International annual meeting poster abstract.

Boyer, J.S. 1982. Plant productivity and environment. Science 218(4571): 443–8.

Brim, C.A. 1966. A modified pedigree method of selection in soybeans. Crop Sci 6: 220.

Broman, K.W., H. Wu, S. Sen, and G.A. Churchill. 2003. R/qtl: QTL mapping in experimental crosses. Bioinformatics 19(7): 889–890.

Brown, J.C. 1963. Iron chlorosis in soybeans as related to the genotype of rootstock. Soil Sci. 96(6): 387–394.

Brown, J.C., and J.E. Ambler. 1973. “Reductants” Released by Roots of Fe-Deficient Soybeans1. Agron. J. 65(2): 311.

Brown, J.C., and J.E. Ambler. 1974. Iron-Stress Response in Tomato (Lycopersicon esculentum) 1. Sites of Fe Reduction, Absorption and Transport. Physiol. Plant. 31(3): 221–224.

Brown, J.C., and L.O. Tiffin. 1965. Iron Stress as Related to the Iron and Citrate Occurring in Stem Exudate. Plant Physiol. 40(2): 395–400.

Burkey, K.O., and T.E. Carter. 2009. Foliar resistance to ozone injury in the genetic base of U.S. and Canadian soybean and prediction of resistance in descendent cultivars using coefficient of parentage. F. Crop. Res. 111(3): 207–217.

Carpentieri-Pipolo, V., A.E. Pipolo, H. Abdel-Haleem, H.R. Boerma, and T.R. Sinclair. 2011. Identification of QTLs associated with limited leaf hydraulic conductance in soybean. Euphytica 186(3): 679–686.

Carter Jr, T.E., P.I. De Souza, and L.C. Purcell. 1999. Recent advances in breeding for drought and aluminum resistance in soybean. p. 4–7. *In* Proc. World Soybean Conf. VI Chicago, IL.

Chaney, R.L., J.C. Brown, and L.O. Tiffin. 1972. Obligatory reduction of ferric chelates in iron uptake by soybeans. Plant Physiol. 50(2): 208–213.

Charlson, D. V., T.B. Bailey, S.R. Cianzio, and R.C. Shoemaker. 2005. Molecular Marker Satt481 is Associated with Iron-Deficiency Chlorosis Resistance in a Soybean Breeding Population. Crop Sci. 45(6): 2394.

Charlson, D. V, S. Bhatnagar, C.A. King, J.D. Ray, C.H. Sneller, T.E. Carter, and L.C. Purcell. 2009. Polygenic inheritance of canopy wilting in soybean [Glycine max (L.) Merr.]. Theor. Appl. Genet. 119(4): 587–94.

Charlson, D.., S.. Cianzio, and R.. Shoemaker. 2003. Associating SSR Markers with Soybean Resistance to Iron Deficiency Chlorosis. J. Plant Nutr. 26(10&11): 2267–2276.

Chen, M., Q.-Y. Wang, X.-G. Cheng, Z.-S. Xu, L.-C. Li, X.-G. Ye, L.-Q. Xia, and Y.-Z. Ma. 2007. GmDREB2, a soybean DRE-binding transcription factor, conferred drought and high-salt tolerance in transgenic plants. Biochem. Biophys. Res. Commun. 353(2): 299–305.

Cianzio, S.R. de, and W.R. Fehr. 1980. Genetic control of iron deficiency chlorosis in soybeans. Iowa State J. Res. 54(3): 367–375.

Coulombe, B.A., R.L. Chaney, and W.J. Wiebold. 1984. Use of bicarbonate in screening soybeans for resistance to iron chlorosis. J. Plant Nutr. 7(1-5): 411–425.

Doerge, R.W., and G.A. Churchill. 1996. Permutation Tests for Multiple Loci Affecting a Quantitative Character. Genetics 142(1): 285–294.

Du, W., M. Wang, S. Fu, and D. Yu. 2009. Mapping QTLs for seed yield and drought susceptibility index in soybean (Glycine max L.) across different environments. J. Genet. Genomics 36(12): 721–31.

Durand, J.L., J.E. Sheehy, and F.R. Minchin. 1987. Nitrogenase Activity, Photosynthesis and Nodule Water Potential in Soyabean Plants Experiencing Water Deprivation. J. Exp. Bot. 38(2): 311–321.

Durrett, T.P., W. Gassmann, and E.E. Rogers. 2007. The FRD3-mediated efflux of citrate into the root vasculature is necessary for efficient iron translocation. Plant Physiol. 144(1): 197–205.

Van Egmond, F., and M. Aktaş. 1977. Iron-nutritional aspects of the ionic balance of plants. Plant Soil 48(3): 685–703.

Fan, J.-B., K.L. Gunderson, M. Bibikova, J.M. Yeakley, J. Chen, E. Wickham Garcia, L.L. Lebruska, M. Laurent, R. Shen, and D. Barker. 2006. Illumina universal bead arrays. Methods Enzymol. 410: 57–73.

Fletcher, A.L., T.R. Sinclair, and L.H. Allen. 2007. Transpiration responses to vapor pressure deficit in well watered “slow-wilting” and commercial soybean. Environ. Exp. Bot. 61(2): 145–151.

Garay, A.F., and W.W. Wilhelm. 1983. Root System Characteristics of Two Soybean Isolines Undergoing Water Stress Conditions1. Agron. J. 75(6): 973.

Gibson, L., and G. Benson. 2005. Origin, History, and Uses of Soybean. Iowa State Univ. Dep. Agron.Available at http://www.agron.iastate.edu/courses/agron212/Readings/Soy_history.htm (verified 8 February 2014).

Gibson, A.H., and F.J. Bergersen. 1980. Methods for legumes in glasshouses and controlled environment cabinets. : 139–184.

Gizlice, Z., T.E. Carter, and J.W. Burton. 1994. Genetic Base for North American Public Soybean Cultivars Released between 1947 and 1988. Crop Sci. 34(October): 1143–1151.

Gutierrez-Gonzalez, J.J., S.K. Guttikonda, L.-S.P. Tran, D.L. Aldrich, R. Zhong, O. Yu, H.T. Nguyen, and D.A. Sleper. 2010. Differential expression of isoflavone biosynthetic genes in soybean during water deficits. Plant Cell Physiol. 51(6): 936–48.

H.M., T., B. E., and B. G.D. 1978. Taproot elongation rates of soybeans. Zeitschrift fuer Acker und Pflanzenbau.

Hansen, N.C., M.A. Schmitt, J.E. Anderson, and J.S. Strock. 2003. Iron Deficiency of Soybean in the Upper Midwest and Associated Soil Properties. Agron. J. 95(6): 1595.

Heatherly, L.G., and R.W. Elmore. 2004. Soybeans: Improvement, Production, and Uses. American Society of Agronomy, Crop Science Society of America, and Soil Science Society of America.

Hether, N.H., R.A. Olsen, and L.L. Jackson. 1984. Chemical identification of iron reductants exuded by plant roots. J. Plant Nutr. 7(1-5): 667–676.

Higgins, C.F. 1992. ABC transporters: from microorganisms to man. Annu. Rev. Cell Biol. 8: 67–113.

Holland, J.B. 2007. Genetic architecture of complex traits in plants. Curr. Opin. Plant Biol. 10(2): 156–61.

Holmberg, S.A. 1973. Soybeans for cool temperate climates. Agri Hort. Genet.

Hudak, C.M., and R.P. Patterson. 1995. Vegetative Growth Analysis of a Drought-Resistant Soybean Plant Introduction. Crop Sci. 35(2): 464.

Hufstetler, E.V., H.R. Boerma, T.E. Carter, and H.J. Earl. 2007. Genotypic Variation for Three Physiological Traits Affecting Drought Tolerance in Soybean. Crop Sci. 47(1): 25.

Hyten, D.L., I.-Y. Choi, Q. Song, J.E. Specht, T.E. Carter, R.C. Shoemaker, E.-Y. Hwang, L.K. Matukumalli, and P.B. Cregan. 2010. A High Density Integrated Genetic Linkage Map of Soybean and the Development of a 1536 Universal Soy Linkage Panel for Quantitative Trait Locus Mapping. Crop Sci. 50(3): 960.

Inskeep, W.P., and P.R. Bloom. 1984. A comparative study of soil solution chemistry associated with chlorotic and nonchlorotic soybeans in western Minnesota. J. Plant Nutr. 7(1-5): 513–531.

Jolley, V.D., J.C. Brown, M.J. Blaylock, and S.D. Camp. 1988. A role for potassium in the use of iron by plants. J. Plant Nutr. 11(6-11): 1159–1175.

Jones, I. 2013. QTL Mapping of Iron Deficiency Chlorosis Tolerance in Soybean Using Connected Populations. : 25.

Kabelka, E.A., B.W. Diers, W.R. Fehr, A.R. LeRoy, I.C. Baianu, T. You, D.J. Neece, and R.L. Nelson. 2004. Putative Alleles for Increased Yield from Soybean Plant Introductions. Crop Sci. 44(3): 784–791.

Keryer, E., V. Collin, D. Lavergne, S. Lemaire, and E. Issakidis-Bourguet. 2004. Characterization of Arabidopsis Mutants for the Variable Subunit of Ferredoxin:thioredoxin Reductase. Photosynth. Res. 79(3): 265–74.

King, C.A., L.C. Purcell, and K.R. Brye. 2009. Differential Wilting among Soybean Genotypes in Response to Water Deficit. Crop Sci. 49(1): 290.

Kramer, D., V. Römheld, E. Landsberg, and H. Marschner. 1980. Induction of transfer-cell formation by iron deficiency in the root epidermis of Helianthus annuus L. Planta 147(4): 335–9.

Kushnir, S., E. Babiychuk, S. Storozhenko, M.W. Davey, J. Papenbrock, R. De Rycke, G. Engler, U.W. Stephan, H. Lange, G. Kispal, R. Lill, and M. Van Montagu. 2001. A mutation of the mitochondrial ABC transporter Sta1 leads to dwarfism and chlorosis in the Arabidopsis mutant starik. Plant Cell 13(1): 89–100.

Landsberg, E. 1982. Transfer cell formation in the root epidermis: A prerequisite for Fe-efficiency? J. Plant Nutr. 5(4-7): 415–432.

Lin, S., S. Cianzio, and R. Shoemaker. 1997. Mapping genetic loci for iron deficiency chlorosis in soybean. Mol. Breed. 3: 219–229.

Lin, S.F., D. Grant, S. Cianzio, and R. Shoemaker. 2000. Molecular characterization of iron deficiency chlorosis in soybean. J. Plant Nutr. 23(11-12): 1929–1939.

Liu, F., M.N. Andersen, S.-E. Jacobsen, and C.R. Jensen. 2005. Stomatal control and water use efficiency of soybean (Glycine max L. Merr.) during progressive soil drying. Environ. Exp. Bot. 54(1): 33–40.

Liu, F., M.N. Andersen, and C.R. Jensen. 2003. Loss of pod set caused by drought stress is associated with water status and ABA content of reproductive structures in soybean. Funct. Plant Biol. 30(3): 271.

Longnecker, N., and R.M. Welch. 1990. Accumulation of apoplastic iron in plant roots : a factor in the resistance of soybeans to iron-deficiency induced chlorosis? Plant Physiol. 92(1): 17–22.

Lucena, J.J. 2000. Effects of bicarbonate, nitrate and other environmental factors on iron deficiency chlorosis. A review. J. Plant Nutr. 23(11-12): 1591–1606.

Mamidi, S., S. Chikara, R.J. Goos, D.L. Hyten, D. Annam, S.M. Moghaddam, R.K. Lee, P.B. Cregan, and P.E. McClean. 2011. Genome-Wide Association Analysis Identifies Candidate Genes Associated with Iron Deficiency Chlorosis in Soybean. Plant Genome J. 4(3): 154.

Mamidi, S., R.K. Lee, J.R. Goos, and P.E. McClean. 2014. Genome-Wide Association Studies Identifies Seven Major Regions Responsible for Iron Deficiency Chlorosis in Soybean (Glycine max). PLoS One 9(9): e107469.

Marschner, H., V. Römheld, and M. Kissel. 1986. Different strategies in higher plants in mobilization and uptake of iron. J. Plant Nutr. 9(3-7): 695–713.

Mian, M.A.R., D.A. Ashley, and H.R. Boerma. 1998. An Additional QTL for Water Use Efficiency in Soybean. Crop Sci. 38(2): 390.

Mian, M.A.R., M.A. Bailey, D.A. Ashley, R. Wells, T.E. Carter, W.A. Parrott, and H.R. Boerma. 1996. Molecular Markers Associated with Water Use Efficiency and Leaf Ash in Soybean. Crop Sci. 36(5): 1252.

Monteros, M.J., G. Lee, A.M. Missaoui, T.E. Carter, and H.R. Boerma. 2006. Identification and confirmation of QTL conditioning drought tolerance in Nepalese soybean PI471938. p. 5–8. *In* The 11th Biennial conference on the molecular and cellular biology of the soybean, August.

Nielsen, D.C., B.L. Blad, S.B. Verma, N.J. Rosenberg, and J.E. Specht. 1984. Influence of Soybean Pubescence Type on Radiation Balance1. Agron. J. 76(6): 924.

Nordborg, M., and S. Tavaré. 2002. Linkage disequilibrium: what history has to tell us. Trends Genet. 18(2): 83–90.

O'Rourke, J. a, R.T. Nelson, D. Grant, J. Schmutz, J. Grimwood, S. Cannon, C.P. Vance, M. a Graham, and R.C. Shoemaker. 2009. Integrating microarray analysis and the soybean genome to understand the soybeans iron deficiency response. BMC Genomics 10(1): 376.

Olsen, R.A., J.C. Brown, J.H. Bennett, and D. Blume. 1982. Reduction of Fe3+ as it relates to Fe chlorosis. J. Plant Nutr. 5(4-7): 433–445.

Paris, R.L. 2003. Uniform Soybean Tests Southern States.

Payne, R., S. Welham, and S. Harding. 2011. A Guide to REML in GenStat. p. 56–57.

Peiffer, G. a., K.E. King, a. J. Severin, G.D. May, S.R. Cianzio, S.F. Lin, N.C. Lauter, and R.C. Shoemaker. 2012. Identification of Candidate Genes Underlying an Iron Efficiency Quantitative Trait Locus in Soybean. Plant Physiol. 158(4): 1745–1754.

Price, A.L., N.J. Patterson, R.M. Plenge, M.E. Weinblatt, N.A. Shadick, and D. Reich. 2006. Principal components analysis corrects for stratification in genome-wide association studies. Nat. Genet. 38(8): 904–9.

Prohaska, K., and W. Fehr. 1981. Recurrent selection for resistance to iron deficiency chlorosis in soybeans. Crop Sci. (2118): 8–10.

Riederer, M. 2001. Protecting against water loss: analysis of the barrier properties of plant cuticles. J. Exp. Bot. 52(363): 2023–2032.

Ries, L.L., L.C. Purcell, T.E. Carter, J.T. Edwards, and C.A. King. 2012. Physiological Traits Contributing to Differential Canopy Wilting in Soybean under Drought. Crop Sci. 52(1): 272.

Risch, N., and K. Merikangas. 1996. The future of genetic studies of complex human diseases. Science (80-.). 273(5281): 1516–1517.

Rodriquez de Cianzio, S., and W.R. Fehr. 1982. Variation in the Inheritance of Resistance to Iron Deficiency Chlorosis in Soybeans1. Crop Sci. 22(2): 433.

Rogers, E.E., and M. Lou Guerinot. 2002. FRD3, a member of the multidrug and toxin efflux family, controls iron deficiency responses in Arabidopsis. Plant Cell 14(8): 1787–99.

Romheld, V. 1987. Different strategies for iron acquisition in higher plants. Physiol. Plant. 70(2): 231–234.

Romheld, V., and H. Marschner. 1981. Iron deficiency stress induced morphological and physiological changes in root tips of sunflower. Physiol. Plant. 53(3): 354–360.

Römheld, V., and H. Marschner. 1984. Plant-induced pH changes in the rhizosphere of "Fe-efficient" and "Fe-inefficient" soybean and corn cultivars. J. Plant Nutr. 7(1-5): 623–630.

Römheld, V., H. Marschner, and D. Kramer. 1982. Responses to Fe deficiency in roots of "Fe-efficient" plant species. J. Plant Nutr. 5(4-7): 489–498.

Romheld, V., C. Muller, and H. Marschner. 1984. Localization and Capacity of Proton Pumps in Roots of Intact Sunflower Plants. PLANT Physiol. 76(3): 603–606.

De Ronde, J.A., R.N. Laurie, T. Caetano, M.M. Greyling, and I. Kerepesi. 2004. Comparative study between transgenic and non-transgenic soybean lines proved transgenic lines to be more drought tolerant. Euphytica 138(2): 123–132.

Scheibe, R. 1987. NADP ^ -malate dehydrogenase in Cj-plants : Regulation and role of a light-activated enzyme. : 393–400.

Severin, A.J., G.A. Peiffer, W.W. Xu, D.L. Hyten, B. Bucciarelli, J.A. O'Rourke, Y.-T. Bolon, D. Grant, A.D. Farmer, G.D. May, C.P. Vance, R.C. Shoemaker, and R.M. Stupar. 2010. An integrative approach to genomic introgression mapping. Plant Physiol. 154(1): 3–12.

Sinclair, T., and M. Ludlow. 1986. Influence of Soil Water Supply on the Plant Water Balance of Four Tropical Grain Legumes. Aust. J. Plant Physiol. 13(3): 329.

Sinclair, T.R., L.C. Purcell, V. Vadez, R. Serraj, C.A. King, and R. Nelson. 2000. Identification of Soybean Genotypes with N Fixation Tolerance to Water Deficits. Crop Sci. 40(6): 1803.

Sinclair, T.R., and R. Serraj. 1995. Legume nitrogen fixation and drought. Nature 378(6555): 344–344.

Sloane, R.J., R.P. Patterson, and T.E. Carter. 1990. Field Drought Tolerance of a Soybean Plant Introduction. Crop Sci. 30(1): 118.

Soerensen, K.U., R.E. Terry, V.D. Jolley, J.C. Brown, and M.E. Vargas. 1988. The interaction of iron-stress response and root nodules in iron efficient and inefficient soybeans. J. Plant Nutr. 11(6-11): 853–862.

Song, Q., D.L. Hyten, G. Jia, C. V Quigley, E.W. Fickus, R.L. Nelson, and P.B. Cregan. 2013. Development and evaluation of SoySNP50K, a high-density genotyping array for soybean. (T Zhang, Ed.). PLoS One 8(1): e54985.

Specht, J.E., K. Chase, M. Macrander, G.L. Graef, J. Chung, J.P. Markwell, M. Germann, J.H. Orf, and K.G. Lark. 2001. Soybean Response to Water. Crop Sci. 41(2): 493.

Specht, J.E., D.J. Hume, and S.V. Kumudini. 1999. Soybean Yield Potential—A Genetic and Physiological Perspective. Crop Sci. 39(6): 1560.

Specht, J.E., J.H. Williams, and D.R. Pearson. 1985. Near-Isogenic Analyses of Soybean Pubescence Genes1. Crop Sci. 25(1): 92.

Stacey, M.G., A. Patel, W.E. McClain, M. Mathieu, M. Remley, E.E. Rogers, W. Gassmann, D.G. Blevins, and G. Stacey. 2008. The Arabidopsis AtOPT3 protein functions in metal homeostasis and movement of iron to developing seeds. Plant Physiol. 146(2): 589–601.

Stocker, T.F., D. Qin, G.-K. Plattner, M. Tignor, S.K. Allen, J. Boschung, A. Nauels, Y. Xia, V. Bex, and P.M. Midgley. 2013. Climate change 2013: The physical science basis. Intergov. Panel Clim. Chang. Work. Gr. I Contrib. to IPCC Fifth Assess. Rep. (AR5)(Cambridge Univ Press. New York).

Tanaka, Y., K. Fujii, and T. Shiraiwa. 2010. Variability of Leaf Morphology and Stomatal Conductance in Soybean [(L.) Merr.] Cultivars. Crop Sci. 50(6): 2525.

Terry, R.E., and V.D. Jolley. 1994. Nitrogenase activity is required for the activation of iron-stress response in iron-inefficient T203 soybean. J. Plant Nutr. 17(8): 1417–1428.

Terry, R.E., K.U. Soerensen, D. Jolley, and J.C. Brown. 1991. The role of active Bradyrhizobium japonicum in iron stress response of soybeans. Plant Soil 130(1-2): 225–230.

Tiffin, L.O., and J.C. Brown. 1959. Absorption of Iron from Iron Chelate by Sunflower Roots. Science 130(3370): 274–5.

Turner, N.C., G.C. Wright, and K.H.M. Siddique. 2001. Adaptation of grain legumes (pulses) to water-limited environments. Adv. Agron. 71: 194–233.

Vaucheret, H. 2008. Plant ARGONAUTES. Trends Plant Sci. 13(7): 350–8.

Wang, J., P.E. Mcclean, R. Lee, R.J. Goos, and T. Helms. 2008. Association mapping of iron deficiency chlorosis loci in soybean (Glycine max L . Merr .) advanced breeding lines. Theor. Appl. Genet. TAG 116(6): 777–787.

Weisenseel, M.H., a Dorn, and L.F. Jaffe. 1979. Natural H Currents Traverse Growing Roots and Root Hairs of Barley (Hordeum vulgare L.). Plant Physiol. 64(3): 512–518.

Weiss, M.G. 1943. Inheritance and Physiology of Efficiency in Iron Utilization in Soybeans. Genetics 28(3): 253–68.

Westgate, M.E., and C.M. Peterson. 1993. Flower and Pod Development in Water-Deficient Soybeans (Glycine max L. Merr.). J. Exp. Bot. 44(1): 109–117.

Woeste, K.E., and J.J. Kieber. 2000. A Strong Loss-of-Function Mutation in RAN1 Results in Constitutive Activation of the Ethylene Response Pathway as Well as a Rosette-Lethal Phenotype. 12(March): 443–455.

Yu, J., G. Pressoir, W.H. Briggs, I. Vroh Bi, M. Yamasaki, J.F. Doebley, M.D. McMullen, B.S. Gaut, D.M. Nielsen, J.B. Holland, S. Kresovich, and E.S. Buckler. 2006. A unified mixed-model method for association mapping that accounts for multiple levels of relatedness. Nat. Genet. 38(2): 203–8.

Zhang, J., H.T. Nguyen, and A. Blum. 1999. Genetic analysis of osmotic adjustment in crop plants. J. Exp. Bot. 50(332): 291–302.